

Stratigraphy of the Chalk Group, Beek04 Borehole, South
Limburg, The Netherlands

Mutaz Alsaif

MSc Thesis (Final Draft)

Department of Earth Sciences – Utrecht University

August 2024

Supervised by: João P. Trabucho Alexandre - Mateus Kroth

Abstract

The Upper Cretaceous deposits of the Chalk Group have been a subject of investigation since the 1800s. They are of great importance to the region of South Limburg, the Netherlands. The Chalk Group aquifers are used for the extraction of groundwater in the region. Recently, the groundwater quality has deteriorated over the years from contamination related to urban activity. The current subsurface geological model doesn't accurately represent the geology of South Limburg as it is not entirely well defined due to the lack of sedimentology studies which in return affects the groundwater safety measures needed to control the quality of the groundwater in the subsurface. In order to understand the depositional evolution and lithofacies changes within the Chalk Group formations in South Limburg, the Roer Valley Graben influence on the deposits of the Chalk Group has to be studied. I studied the data from Beek04 borehole located in the western part of South Limburg. The study encompasses lithofacies analysis, microfacies characterization, integration with wireline logs, and identification of aquifers' properties using petrophysical data. The results from this study were correlated with the Eys01 borehole located in the eastern part of South Limburg to assess the influence of the Roer Valley graben inversion and lateral continuity of the Chalk Group formations in the area of interest. The main outcome of this research is that the Beek04 borehole recovered the Gulpen Formation contrary to the current interpretation found in DINOLOket DGM model which assumes that the Gulpen Formation is entirely missing in Beek04 borehole. This finding marks the first step towards improving the current subsurface geological model in South Limburg which in return can be used to improve the (hydro)stratigraphic model of the region.

1. Introduction

Upper Cretaceous deposits of the Chalk Group have been a subject of investigation since the 1800s (e.g., Fitton, 1834; Dumont, 1849). They have economic significance as they have been used for oil and gas exploration in the North Sea (Megson et al., 2005) or flint mining in the southern part of the Netherlands (Boyston et al., 2023). In the region of South Limburg, the Chalk Group aquifers have been used for the extraction of groundwater. However, the quality of the groundwater has deteriorated by nitrate and pesticides from nearby urban activity over the years (Van Maanen et al., 2001). In order to implement groundwater safety measures, an updated geological model of the subsurface is needed as the current subsurface model does not accurately represent the architecture and distribution of the Chalk Group in the region.

The region of South Limburg is situated between the Roer Valley Graben, to the north, and the Rhenish Massif, to the south (Fig. 1). In the Late Cretaceous, this region has been affected by tectonic events and sea level fluctuations that shaped and influenced the geology of the area (Bless et al., 1986; Gras & Geluk, 1995). The Roer Valley Graben underwent inversion during the Subhercynian tectonic phase of Santonian to Campanian age (Van Wijhe, 1987a, b; Geluk et al., 1994; Nalpas et al., 1996; Gras & Geluk, 1999). During that time, the Chalk Group was deposited as a consequence of a transgression along the northern edge of the Brabant Massif (Felder & Bosch, 2000; Herngreen, 2007). The Chalk Group was deposited in the more proximal part of the Chalk Sea, which flooded the northwest of Europe during the Late Cretaceous (Mortimore, 2018). The interplay between sedimentation and tectonics resulted in heterogeneities of the Chalk Group formations in the area of interest.

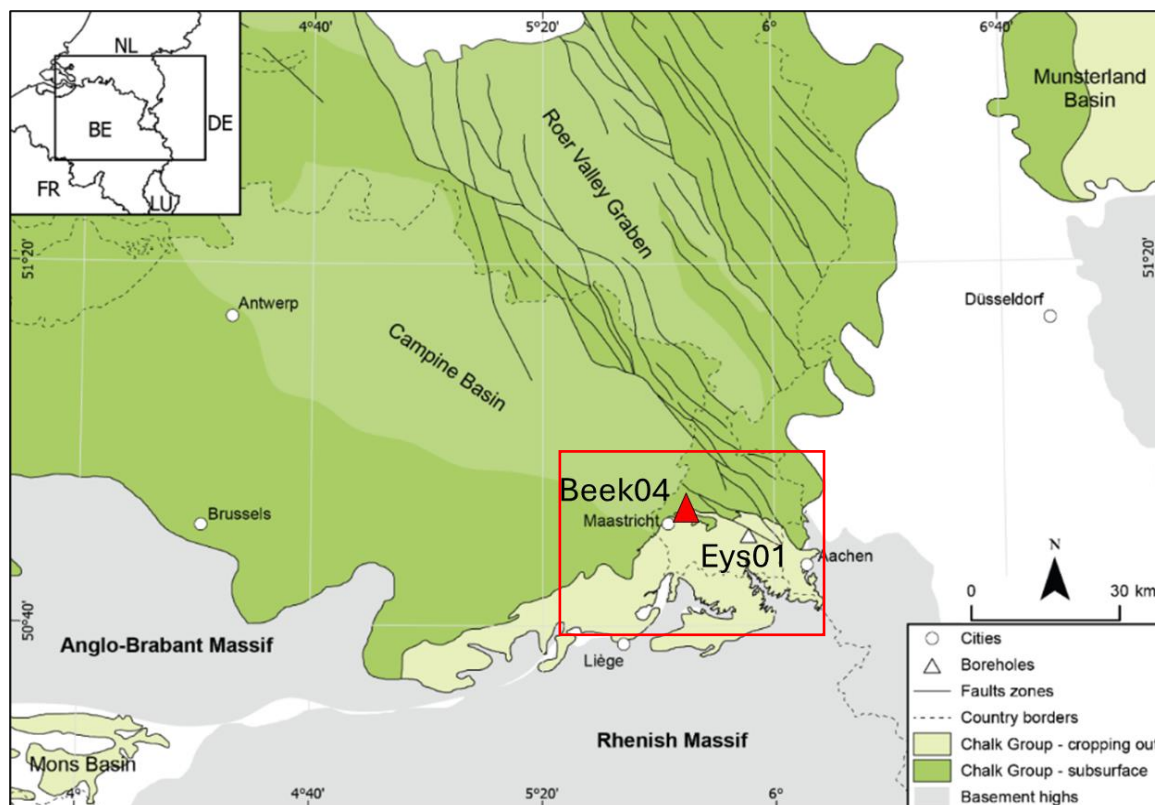


Fig. 1: Location map of South Limburg highlighted in the red box, showing the distribution of The Chalk Group deposits in NW Europe, structural elements, and location of boreholes as triangles (Beek04 in red – Eys01 in white)

The Chalk Group is traditionally subdivided into five formations: Aken (siliciclastic dominated), Vaals (siliciclastic dominated), Gulpen (mixed siliciclastic and carbonate), Maastricht (carbonate dominated), and Houthem formations (carbonate dominated), (Felder & Bosch, 2000). The Maastricht Formation was informally subdivided into two facies, Maastricht (in the west) and Kunrade facies (in the east). However, Kroth et al., (2024) suggested that the Kunrade facies should be afforded the status of formation as it is a mappable unit that displays significant differences when compared with the Maastricht facies. (Fig. 2).

	Age	Formation		Tectonic Event
Paleogene	Danian	Houthem		Laramide Inversion
		Maastrichtian	Maastricht	
Late Cretaceous	Campanian		Gulpen	
		Vaals		
		Aken		
	Santonian			

Fig. 2: Lithostratigraphic subdivision of the Chalk Group (Felder & Bosch, 2000; Kroth et al., 2024)

In order to understand the architecture and distribution of the Chalk Group in the region, the influence of the Roer Valley Graben on the sedimentation of the Chalk Group needs to be investigated. According to Bless et al., (1986), the inverted Roer Valley Graben is considered to have been a source of siliciclastic material to the region of South Limburg. Thus, creating heterogeneities in the deposits of the Chalk Group. Based on that, Felder (1975), Felder (1985) and Felder & Bosch (2000) proposed an informal east-west subdivision of the formations of the Chalk Group in South Limburg.

A product of **this** inversion is the pre Valkenburg strata. Those deposits were introduced by Felder (1985) using the term “pre-Valkenburg strata” to describe the transitional facies characterized by marly, glauconitic sands and silts found in between the Vaals and Maastricht formations. The pre-Valkenburg strata is equivalent to the Gulpen Formation. It was observed in South Limburg and is associated with areas that are affected by faults (Felder, 1985). According to Jagt et al., (1987), the pre-Valkenburg strata contains erosional products associated with the inverted Roer Valley Graben. Thus, more siliciclastic material is expected in the Gulpen Formation around the inverted Roer Valley Graben. In opposite to the southern part of South Limburg where the Gulpen Formation was studied (e.g., the ENCI and Hallembaye quarries) and is mainly composed of finer grained chalk deposits with minor siliciclastic material (Vellekoop et al., 2022).

To study the impact of the Roer Valley Graben inversion in South Limburg, I studied the Beek04 borehole located in the northwestern part and correlated it with the Eys01 borehole located in the northeastern part of South Limburg. The location of the boreholes enables the assessment of the east-west lateral continuity of the deposits. In addition, since both boreholes located in the north of South Limburg, in a proximal location to the inverted Roer Valley Graben, comparisons between the northern part of South Limburg with the southern part of South Limburg were made to gain a regional understanding of the heterogeneities of the Chalk Group formations.

In this study, I carried out a lithofacies and microfacies analysis of the cores of the Beek04 borehole. In addition, petrophysical properties of the rocks (e.g., porosity and permeability) were measured from cores and thin sections. This is done to update the stratigraphy of the Beek04 borehole, to gain a regional understanding of the geology of the area and to identify aquifers' properties of the Chalk Group in South Limburg.

The main outcome of this study is that the Beek04 borehole recovered the Gulpen Formation, which doesn't agree with the current interpretation found in Dinoloket DGM model (Fig. 3) where the Gulpen Formation is assumed to be entirely missing in the borehole. Such discrepancies in identifying

formations in the subsurface limit the accuracy of the (hydro)stratigraphic model in South Limburg which in return affects the groundwater safety measures needed to solve the problem. Thus, the generated petrophysical properties of the formations of the Chalk Group (table 1) can be used with the updated lithostratigraphic division of the Beek04 borehole to update the (hydro)stratigraphic model in South Limburg.

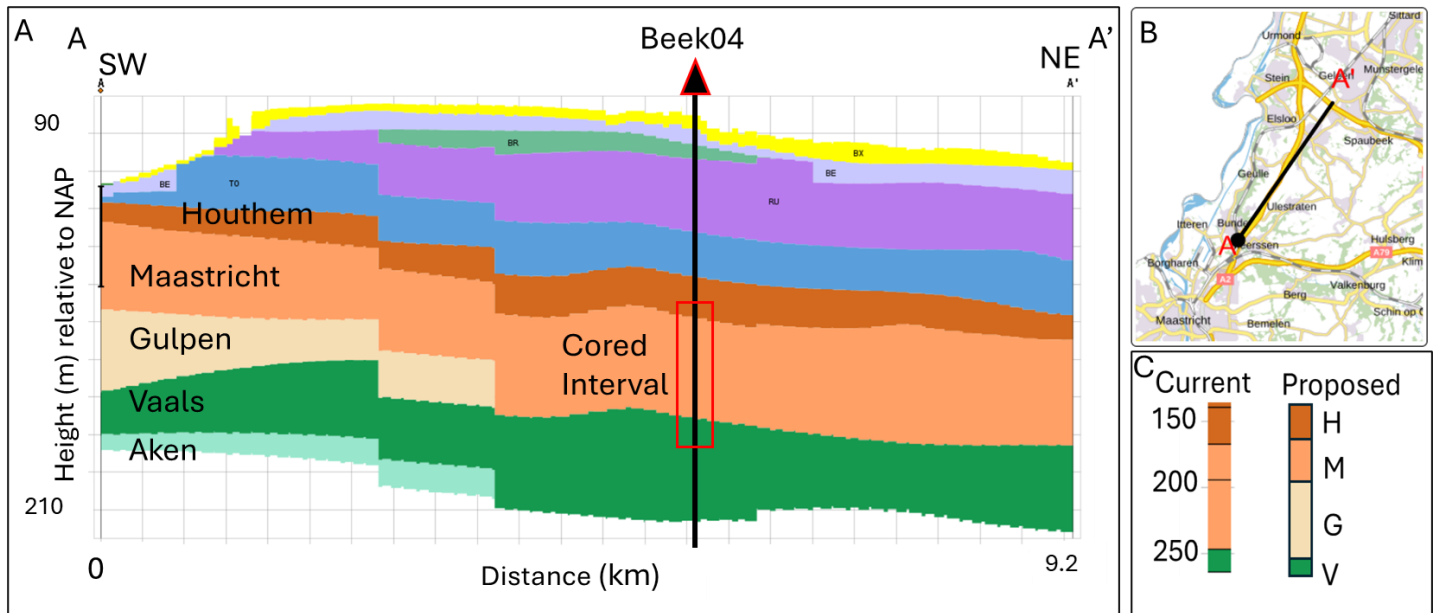


Fig. 3: **A)** Subsurface model obtained from DINOLOKET DGM model for cross section (A-A') with the location of Beek04 borehole and the cored interval highlighted in the red box. The current geological model assumes that entire Gulpen Formation is missing in the Beek04 borehole with a considerably thicker Maastricht Formation succession than observed in the SW. **B)** Location map of cross section (A-A'). **C)** Compares the current subdivision of the Beek04 borehole versus the proposed subdivision from this study which suggests the deposition of the Gulpen Formation in Beek04 borehole.

2. Materials and Methods

In this research, I studied the data obtained from cores of the Beek04 borehole. The borehole was drilled in 1983 by Shell. It is located in South Limburg, in the Maastricht airport terrain with the following UTM coordinates 31U (694938, 5644750). The total depth of the borehole is 263.85 m and the elevation is 110.5 m.

2.1 Beek04 Cores

The cored interval (147.2–264 m) corresponds to Vaals, Gulpen, Maastricht and Houthem formations. The cores were cut from a vertical borehole drilled normal to bedding. I studied the cored interval from (264-167 m), disregarding the upper part of the core from (167-147.2 m) due to the state of the cores, as I observed missing sections and poor recovery rate (16.7%).

2.2 Core Description

The core description was used to identify lithofacies and to understand the vertical succession of the Chalk Group in this locality. I described the cores focusing on grain size, composition, bioturbation and color.

For the grain size description, I used Wentworth (1922) grain size classification scheme to describe changes in the grain size of the rocks. As for the composition of the rocks, I adapted a modified version of Macquaker & Adams (2003) classification scheme which uses the term “dominated” if the rock contains more than 90% of the same material, the term “rich” if the rock contains 50-90% of the same material, the term “bearing” if the rock contains 50-10% of the same material, the term “minor” if the rock contains 5-10% of the same material and finally, the term “rare” if the rock contains 0-5% of the same material.

Bioturbation was characterized using the bioturbation intensity index of Droser & Bottjer (1986), which ranges from 1 (no bioturbation observed) to 6 (bedding is homogenized). Lastly, I used Campbell, (1967) terminology to describe the lamina and bed thickness and texture.

2.3 Sampling Strategy

I collected a total of 49 samples across the cored interval. The samples were used for petrography analysis at a maximum distance of 3 m between samples with more dense sampling intervals throughout the core in key locations corresponding to facies change (see Fig. 4 for sample locations and density).

2.4 Thin Sections

The samples were prepared by Wagner Petrographic. The samples' slide thickness is 30 μm thick with Alizarin red staining to detect and distinguish calcite from dolomite and impregnated with blue epoxy to identify porosity.

I described the thin sections qualitatively focusing on grain type, grain size, texture using Dunham (1962) for carbonate rocks, roundness, sorting, as

well as the presence of cement, mud, fractures, bioturbation and porosity. Also, semi-quantitative description was performed by visually estimating the relative percentage of each component found in the samples. The thin sections were used to aid in identifying microfacies and investigate pore types and distribution as well as cement presence in the rocks.

2.5 Porosity Estimation

Porosity was described using Choquette and Pray's method (1970) and estimated quantitatively by image analysis. ImageJ software was used for this purpose. A 10×15 mm rectangle from the thin section was chosen, after which I used color thresholds that best matched the color of the blue-dyed epoxy in pore spaces. The porosity was calculated by dividing the sum of the entire area of selected pores by the total area of the rectangle. To quality check the results, I compared the shape (morphology) and size of the porosity polygons generated by the software with the original porosity of the micrograph. In addition, I measured porosity three times for each thin section with an average error of $\pm 3\%$.

2.6 Logs Data

The data set obtained from the borehole includes gamma ray and resistivity wireline logs that were used to correlate the data from Beek04 to nearby boreholes (Eys01). In addition, a horizontal permeability log was measured from the core with a 30 cm spacing between measurements to gain a better understanding of the aquifer's properties. The measurements were done using NER's TinyPerm device which is a handheld air permeameter used to measure rocks' matrix permeability.

2.7 Correlation with Eys01 Borehole

The Eys01 borehole was studied by Kooij, (2023). Observations made on the Eys01 cores will be compared with observations made on the cores of the Beek04 borehole. The Eys01 borehole is located in the east of South Limburg, in a proximal location relative to the Roer Valley Graben. Thus, both the influence of the Roer Valley Graben and the lateral heterogeneities of the Chalk Group formations were investigated to gain a regional understanding of the subsurface geology.

3. Results

3.1 Description of the Beek04 borehole

A total of 93.5 m of cores were described from the Beek04 borehole. The studied cored interval is from 264 m to 167 m with a 96.5% recovery rate. In general, the Beek04 borehole can be subdivided into three intervals, siliciclastic dominated interval in the bottom of the cores, mixed siliciclastic and carbonate interval in the middle of the cores and a pure carbonate interval in the upper part of the cores (Fig. 4).

The bottom part of the cores from 264 to 246 m is a siliciclastic dominated interval that is made up of two coarsening upward cycles of sandy glauconite bearing siltstones grading into very fine to fine glauconite bearing sandstone which are overlain by a breccia towards the uppermost part of the interval. Skeletal fragments and bivalves were observed as well in the interval between 264-246 m. Three lithofacies (A1-A3) were identified in the succession (264-246) m. In addition, wireline logs are showing different logs signatures for this interval when compared to the rest of the cores. It shows a higher gamma ray signature than the carbonate intervals (Fig. 4).

The contact between the siliciclastic dominated interval and the overlying mixed siliciclastic and carbonate interval is unconformable and characterized by an abrupt change in lithology (Fig. 5). The upper 6 cm of the siliciclastic dominated interval is composed of breccia (A3) that is followed by a cemented limestone (B1) (Fig. 5C) found at the base of the mixed siliciclastic and carbonate interval. In addition, microfacies unit M3 in the upper part of the siliciclastic dominated interval contains medium to very coarse, rounded quartz grains mixed in a matrix composed of very fine to fine, angular to sub-angular quartz grains (Fig. 5B).

The interval from 246 m to 192 m consists of mixed siliciclastic and carbonate rocks interbedded with siliciclastic rocks in the bottom part, cleaning upwards to a more carbonates dominated deposits towards the top of the interval. It is made up of very fine to fine, bioturbated calcarenites. The calcarenites can be subdivided in two facies units based on cementation. One unit is soft, partly cemented with minor quartz and glauconite content. The other unit is indurated, cemented with rare quartz and glauconite content. Bivalves, bryozoans, skeletal fragments were observed in the calcarenites. In addition, laminated, glauconite bearing, very fine to fine sandstones are interbedded with the calcarenites. This interval contains flint nodules that are mostly found in the highly cemented intervals. Flint nodules are dark grey, 2-5 cm thick and have an irregular shape in the bottom part of the interval. Flint nodules in the upper part are weakly developed, more abundant and less extensive with light grey color. I identified 4 facies (B1-B4) in this part of the core. Moreover, looking at the

wireline logs signature of this interval. It shows lower gamma ray and permeability values when compared to the siliciclastic dominated part of the core (Fig. 4).

The contact between the overlying pure carbonate interval and the mixed siliciclastic and carbonate interval in Beek04 appears to be gradual and occurs over an approximately 10 meters interval. The deposits towards the upper part of the mixed siliciclastic and carbonate interval show a decrease in the bioturbation index as well as a decrease of glauconite and siliciclastic content to almost equals zero (Fig. 6).

This interval in the upper part of the core from 192 to 167m is composed of pure carbonate deposits with rare siliciclastic input that makes up less than 1% of the rocks. It is composed of partially cemented, fine to medium calcarenites with fossil layers. In addition, a 30 cm muddy calcarenite was observed at depth of 174 m. Lastly, the uppermost part of the cores is made up of 2 meters thick, very soft (friable) calcarenite. Flint nodules are light grey and only appear in the bottom half of the interval. Four lithofacies (C1-C4) were identified in this part of the cores. In addition, this interval shows the cleanest gamma ray log signature and the highest permeability and porosity values. Also, we notice that the resistivity logs show separation in the values when comparing the three resistivity logs and this can be related to the high porosity and permeability values (Fig. 4).

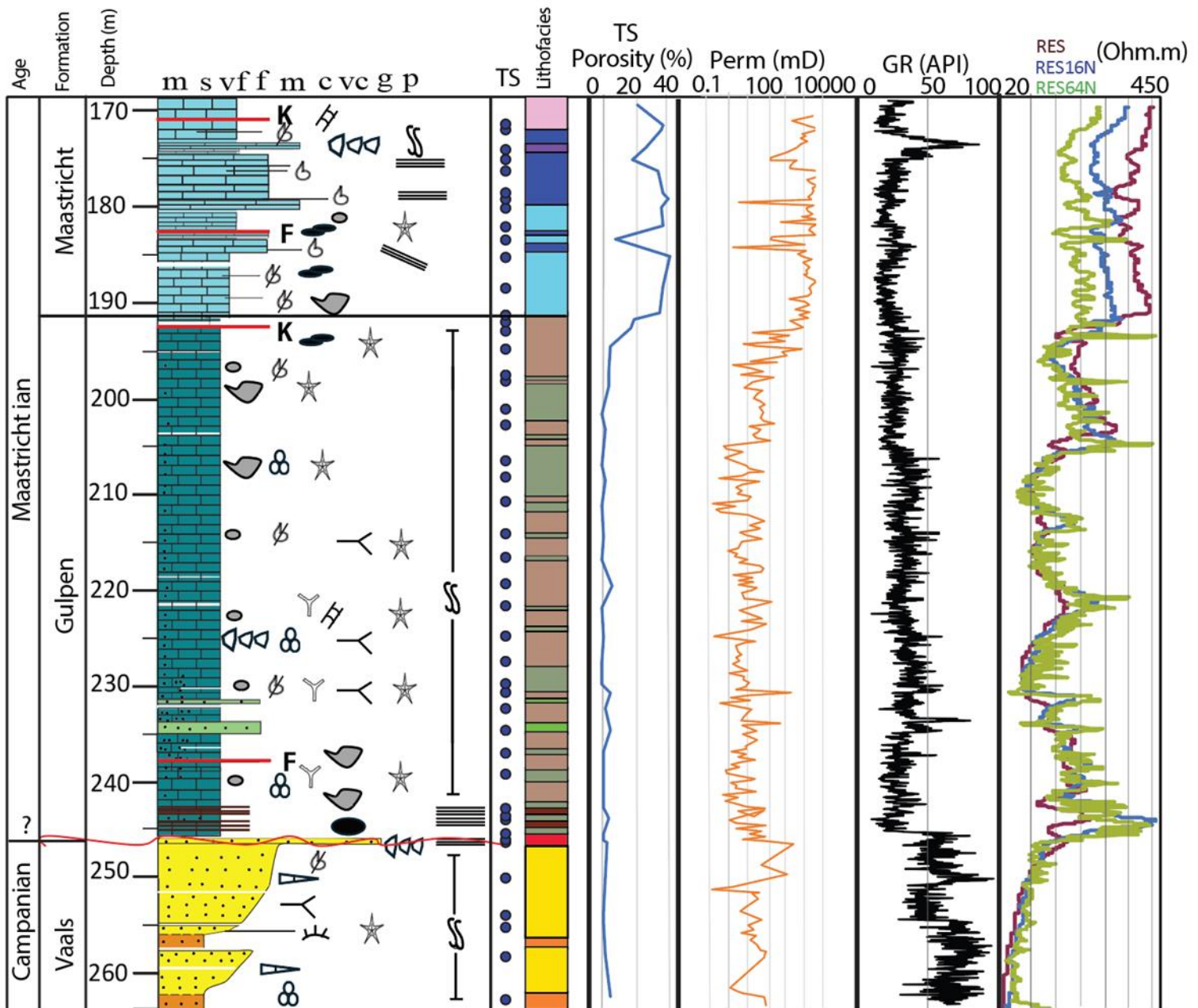


Fig. 4: Master log of Beek04 borehole showing core description, thin section locations, lithofacies subdivision, porosity measured from thin sections, permeability log measured from the core, GR log and resistivity logs (shallow, medium and deep). The cored interval can be subdivided into three main intervals: 1- siliciclastic dominated interval in bottom of the core. 2- mixed carbonate and siliciclastic interval in the middle of the core 3- pure carbonate interval in the upper part of the core. The subdivision can also be observed in all the plotted logs. Note: legend for the Fig. is in (Appendix A)

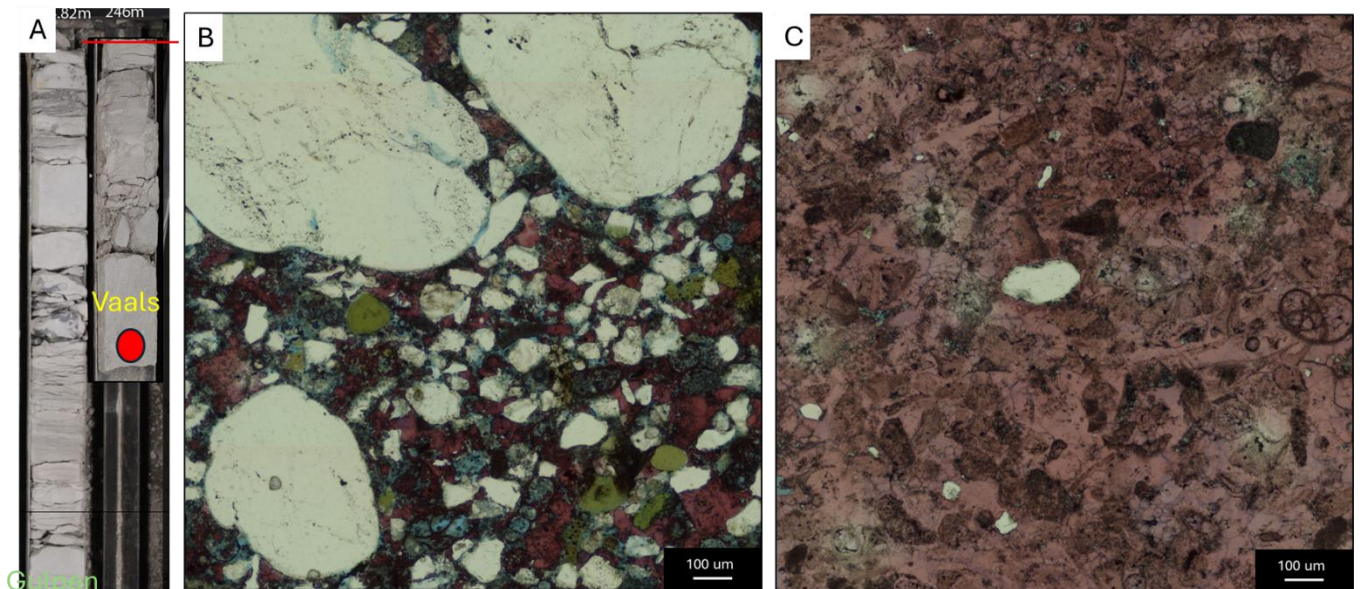


Fig. 5: A) Core photos showing the contact between Vaals (siliciclastic dominated) and Gulpen (mixed carbonate and siliciclastic) formations marked by the red line at 246 m on top of box 105. Red circles highlight the position of the thin section shown in B&C. B) Microfacies M3 in the upper part of the Vaals Formation contains medium to very coarse, rounded quartz grains mixed in a matrix composed of very fine to fine, angular to sub-angular quartz grains. C) Microfacies M4 showing cemented carbonate rocks with rare quartz grains. Note the abrupt change in lithology between the two formations.

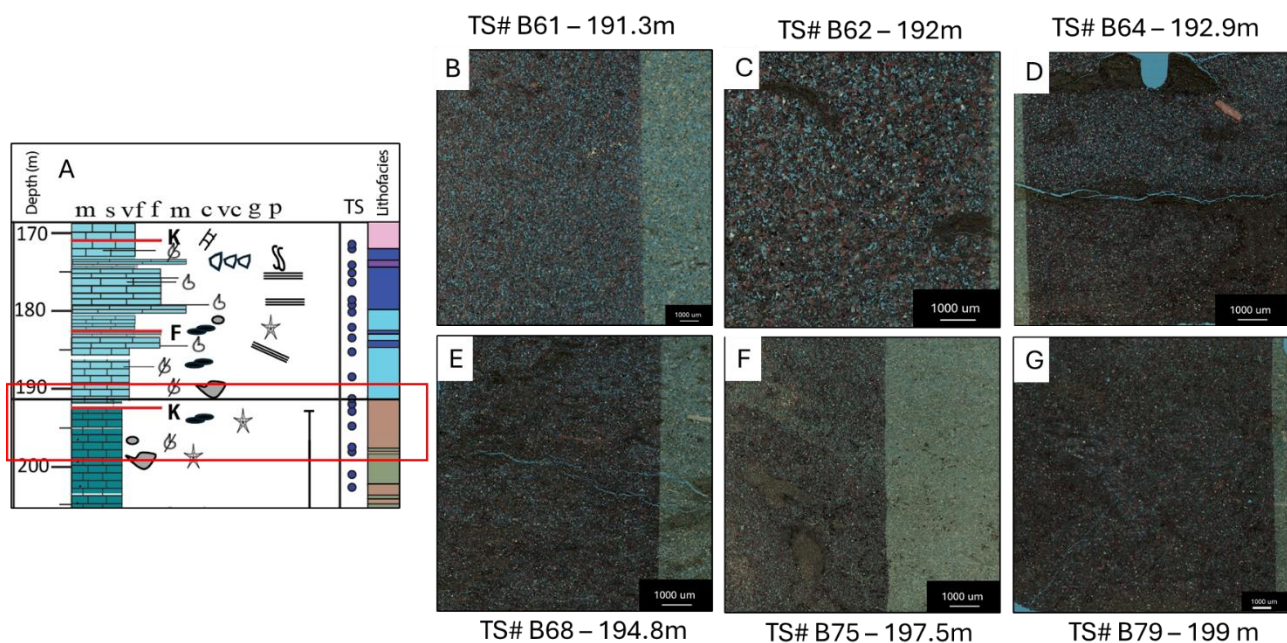


Fig. 6: Showing the contact between the Gulpen (mixed carbonate and siliciclastic) and Maastricht (pure carbonate) formations in the Beek04 borehole. A) Core description log showing the location of the thin section shown in Figs (B to G) and the contact between the two formations represented by the color change in the lithology column marked at 191.5 m. G to B) Note the decrease in bioturbation index from BI:5 to BI:0 and the decrease in glauconite and siliciclastic content from 10% to almost zero as we move from Fig. G (deepest) to Fig. B (shallowest). In addition, these changes are accompanied by an increase in porosity and permeability. B) marking the appearance of the Maastricht Formation in the Beek04 borehole characterized by the presence of pure carbonate deposits. The contact appears to be gradual and occurs over approximately 10 m interval.

3.1.1 Lithofacies

In total, 11 lithofacies were described in the Beek04 cores. Facies A represents the siliciclastic dominated interval in the bottom part of the core. Facies B represents the mixed siliciclastic and carbonate interval in the middle of the core. Finally, Facies C represents the pure carbonate deposits in the upper part of the core.

A1 – Bioturbated glauconite bearing siltstone.

Facies A1 is characterized by a light to dark grey, bioturbated (BI:2) glauconite bearing siltstone. Bivalve shells both broken and whole with random orientation were observed in the rocks. Also, skeletal fragments and belemnites are present. The thickness of this facies is around 2 meters, and it makes the bottom part of two coarsening upward sequences observed in the siliciclastic dominated interval (Fig. 7A).

A2 – Bioturbated glauconite bearing very fine sandstone.

This facies is described as a brownish light grey to grey, very fine to fine bioturbated (BI:2) glauconite bearing sandstone. The rocks show an alternation between indurated (less muddy) and soft (muddier) intervals. I observed the same fossils as in facies unit A1 but in less amounts. Facies A2 maximum thickness is around 8.5 m, it overlies facies A1 and makes the upper part of the coarsening upward sequences that were observed in the siliciclastic dominated interval (Fig. 7C).

A3 – Glauconite bearing breccia.

Facies A3 is characterized by a grey, medium to coarse poorly sorted, glauconite bearing breccia. The matrix of the rock is made up of glauconite bearing sandstone with rare skeletal fragments. The breccia is overlain by a 2 cm laminated very fine sandstone where medium to coarse lithoclasts of the laminated rock were eroded and redeposited in different orientations (Fig. 7E). The thickness of facies A3 is approximately 0.3 m, and it makes the upper most part of the siliciclastic dominated interval (Fig. 7E).

B1 – Indurated very fine calcarenites.

Facies B1 can be described as off white to light grey cemented very fine to fine calcarenites, indurated, bioturbated in part (BI:2) with intervals of dark to light grey flint concentrations. Skeletal fragments, (e.g., bryozoans and echinoderm spines) were observed in this facies with rare quartz and glauconite content. This facies is observed across the whole mixed interval with maximum thickness of 0.5 m (Fig. 8A).

B2 – Soft very fine calcarenites.

Facies B2 is made up of tan to light grey, partially cemented, very fine to fine calcarenites, soft, bioturbated with intervals of weakly developed flint concentrations. Skeletal fragments, (e.g., echinoderm spines) are observed in this facies unit with minor quartz and glauconite content. Facies B2 has a maximum thickness of approximately 1 m and is observed across the mixed interval alternating with facies unit B1 (Fig. 8C).

B3 - Laminated fine sandstone with glauconitic muddy matrix

Facies B3 is comprised of grey, to dark grey, very fine to fine glauconite bearing sandstone with glauconitic muddy matrix, moderately sorted, soft, with rare skeletal fragments. B3 is horizontally laminated and the average thickness of facies B3 is approximately 5 cm with a thickness ranging from 2-10 cm. Facies B3 is found in the bottom part of the mixed interval (Fig. 8E).

B4 – Very fine greensand

Facies B4 is characterized by a greenish grey, to dark grey, very fine to fine greensand. It is well sorted, soft and glauconite bearing. The maximum thickness of this facies is 1.3 m between 235.5 m and 234.1 m and is found in the lower part of the mixed interval (Fig. 8H).

C1 – Indurated, very fine calcarenites.

Facies C1 can be described as off white to tan, very fine calcarenite, indurated, with intervals of light grey flint concentrations. Skeletal fragments are observed in this facies as well as fossil layers. Quartz and glauconite content decreased to almost zero. Facies C1 makes up most of the pure carbonate interval, its thickness is up to 25 m. The rocks display high porosity values up to 20-30% (Fig. 9A).

C2 – Soft, fine to medium calcarenites

Facies C2 can be described as light brown, soft, fine to medium calcarenite, with intervals of light grey flint concentrations. Skeletal fragments are observed in this facies unit as well as fossil layers. Quartz and glauconite content decreased to almost zero. The depth interval (176.8 -176.5 m) is cross bedded (Fig. 15A) and will be given the code C2A. Visible porosity ranging from (5-10%). Facies unit C2 alternates with facies C1. (Fig. 9C)

C3 – Bioturbated, laminated, muddy very fine calcarenite.

This facies is made up of greyish brown, laminated, bioturbated (BI:4) muddy, poorly sorted, very fine calcarenite with rare skeletal fragments up to cm size and rare intraclasts. Facies C3 is 0.3 m thick and can be found in the depth range between 174.3-174 m. (Fig. 9E)

C4 – Friable very fine calcarenite

Facies C4 is characterized by white to off-white, very fine to silt calcarenites with rare skeletal fragments such as bivalves up to 2 cm in size and rare intraclasts. This facies occurs only in the upper most part of the core. Its thickness is approximately 2 meters. (Fig. 9H)

4.1.2 Microfacies

In total, 11 microfacies were described in the Beek04 cores. Microfacies (M1-M3) represent the siliciclastic dominated interval in the bottom part of the core. Microfacies (M4-M7) represent the mixed siliciclastic and carbonate interval in the middle of the core. Finally, microfacies (M8-M11) represent the pure carbonate deposits in the upper part of the core.

M1 – Bioturbated glauconite bearing siltstone.

Glauconite bearing siltstone, moderately sorted, angular to sub-angular with minor very fine quartz content. Bioturbated (BI:2) with muddy matrix. The rock contains minor silt sized bioclasts, mainly skeletal fragments, bivalves and foraminifera. Glauconite pellets are dispersed in the rock. Porosity is primary (intercrystallite) and secondary (moldic). Also, open fractures are observed in this facies (Fig. 7B).

M2 - Bioturbated glauconite bearing very fine sandstone.

glauconite bearing sandstone, angular to sub-angular with minor medium quartz content. Bioturbated (BI:2-3) with burrows filled mainly with mud and bioclasts. The rock can be bioclast bearing with mainly, skeletal fragments, echinoderm, bivalves and foraminifera. Porosity is secondary (moldic). Glauconite pellets are dispersed in the rock. This microfacies can be subdivided into two subunits based on the sorting of the rock. Microfacies M2-A is well sorted very fine to fine sandstone, while facies M2-B is poorly sorted very fine to fine sandstone with minor medium quartz content (Fig. 7D).

M3 - Bioturbated glauconite bearing poorly sorted fine sandstone.

glauconite bearing, angular to sub-angular fine sandstone, poorly sorted with coarse to very coarse, sub-rounded quartz and rare intraclasts. Bioturbated (BI:2) with burrows filled mainly with mud and bioclasts. The matrix is muddy and bioclastic mainly skeletal fragments, echinoderm, bivalves and foraminifera with very fine angular to sub-angular glauconite. Porosity is secondary (moldic) and enlarged by dissolution. Glauconite pellets are dispersed in the rock. In addition, calcite cement is present in parts of the thin section (Fig. 7E).

M4 – Cemented bioturbated bioclastic packstone to grainstone.

Cemented bioclastic packstone with rare coarse silt to very fine quartz and glauconite content (0-10%). Bioturbated (BI:1-4), with burrows filled with mud or the original rock texture. The rock contains skeletal fragments, foraminifera, bryozoans and echinoderm spines. Open fractures and partially cemented fractures are observed in thin sections. Blocky calcite replaced the original texture of the rock (Fig. 8B).

M5 – Muddy bioturbated bioclastic packstone.

Muddy bioclastic packstone with minor moderately sorted coarse silt to very fine quartz and glauconite content. Bioturbated (BI:2-5), with burrows filled with quartz and glauconitic mud. The rock contains skeletal fragments, foraminifera, bryozoa, red algae sponge spicules and echinoderm spines.

Open fractures are observed in thin sections. Porosity is primary (intercrystallite) and secondary (moldic) (Fig. 8D).

M6 – Laminated glauconite bearing very fine sandstone.

Laminated (Fig. 8F), glauconite bearing very fine to fine sandstone, moderately sorted, angular to sub-angular with minor silt sized bioclasts. The rock contains a dark grey glauconitic muddy matrix. Porosity is secondary (moldic) and in open fractures. Glauconite pellets are dispersed in the rock. (Fig. 8G).

M7 – Glauconite bearing very fine greensand.

Glauconite bearing very fine to fine greensand, well sorted, sub-angular with rare silt sized bioclasts. Porosity is primary (intercrystallite) and secondary (moldic). Also, open fractures are observed in this facies. Glauconite pellets are dispersed in the rock. The main difference between microfacies M7 and microfacies M2 is that the glauconite content in M7 is almost equal to the quartz content in the rock (Fig. 8I).

M8 – Very fine bioclastic packstone to grainstone.

Very fine to fine packstone to grainstone. The rock contains skeletal fragments, foraminifera, and echinoderm spines. Microfacies M8 is moderately sorted. Minor amount of mud can be present in the matrix. Blocky calcite growing around the bioclasts. Porosity is primary (intercrystallite) and secondary (moldic). Also, open fractures are observed in thin sections (Fig. 9B).

M9 – Fine to medium bioclastic packstone to grainstone.

Very fine to medium packstone to grainstone. The rock contains skeletal fragments, foraminifera, red algae, and echinoderm spines. Microfacies M9 is poorly sorted and contains coarse to very coarse bioclasts with minor amount of mud. Blocky calcite growing around the bioclasts. Porosity is primary (intercrystallite) and secondary (moldic). Also, open fractures are observed in thin sections (Fig. 9D).

M10 – Muddy, laminated, bioturbated, bioclastic grainstone.

Bioclastic, very fine, muddy grainstone. The rock contains skeletal fragments, foraminifera and echinoderm spines. Porosity is primary (intercrystallite) and secondary (moldic). This microfacies unit can be laminated (Fig. 9F) and bioturbated (BI:5) (Fig. 9G).

M11 – Very fine calcarenite

Very fine to fine calcarenite with rare coarse skeletal fragments such as bivalves up to 2 cm in size and rare intraclasts. The laminated parts of the thin section are more compacted when compared to the non-laminated parts (Fig. 9J). The rock is bioturbated BI=2. Open fractures are observed in this unit. (Fig. 9I)

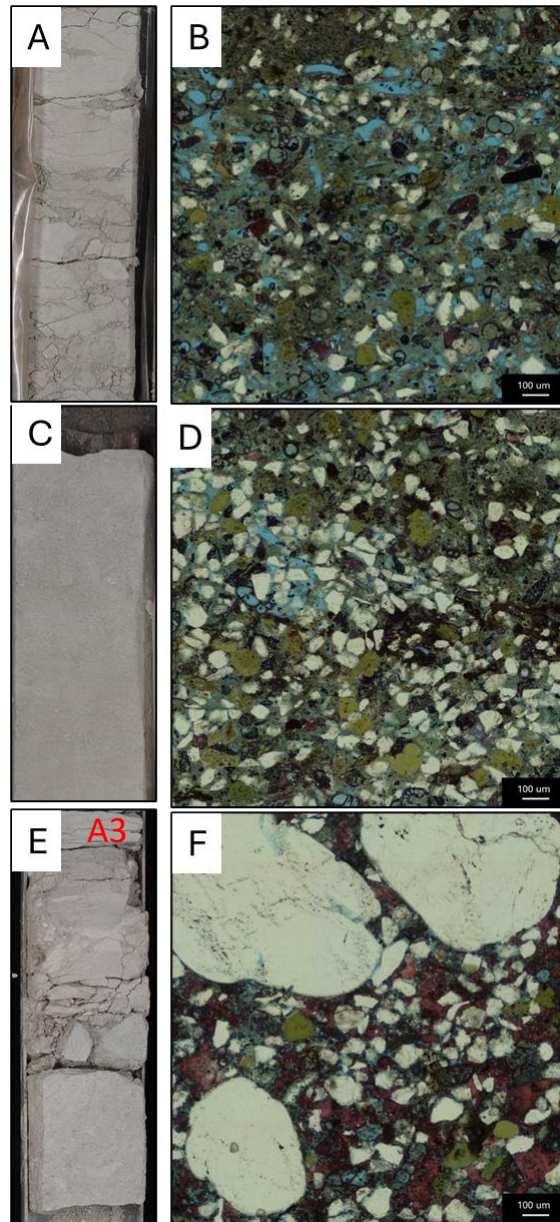


Fig. 7: Facies of the siliciclastic dominated interval (Vaals Fm.) showing bioturbated, bioclastic, glauconitic siliciclastic rocks. The core photos represent lithofacies. Thin sections photos represent microfacies. **A)** A1 (262.7-262.5 m). **B)** M1 associated with lithofacies A1 TS# B236 – 262.7 m BI=3. **C)** A2 (258.7-258.2 m). **D)** M2 associated with lithofacies A2 TS# B226 – 258.4 m BI=3. **E)** A3 (246.3-246.1 m) only the broken part of the core. **F)** M3 **not** associated with lithofacies A3, the sample is taken directly below the broken section TS# B195 – 246.4 m.

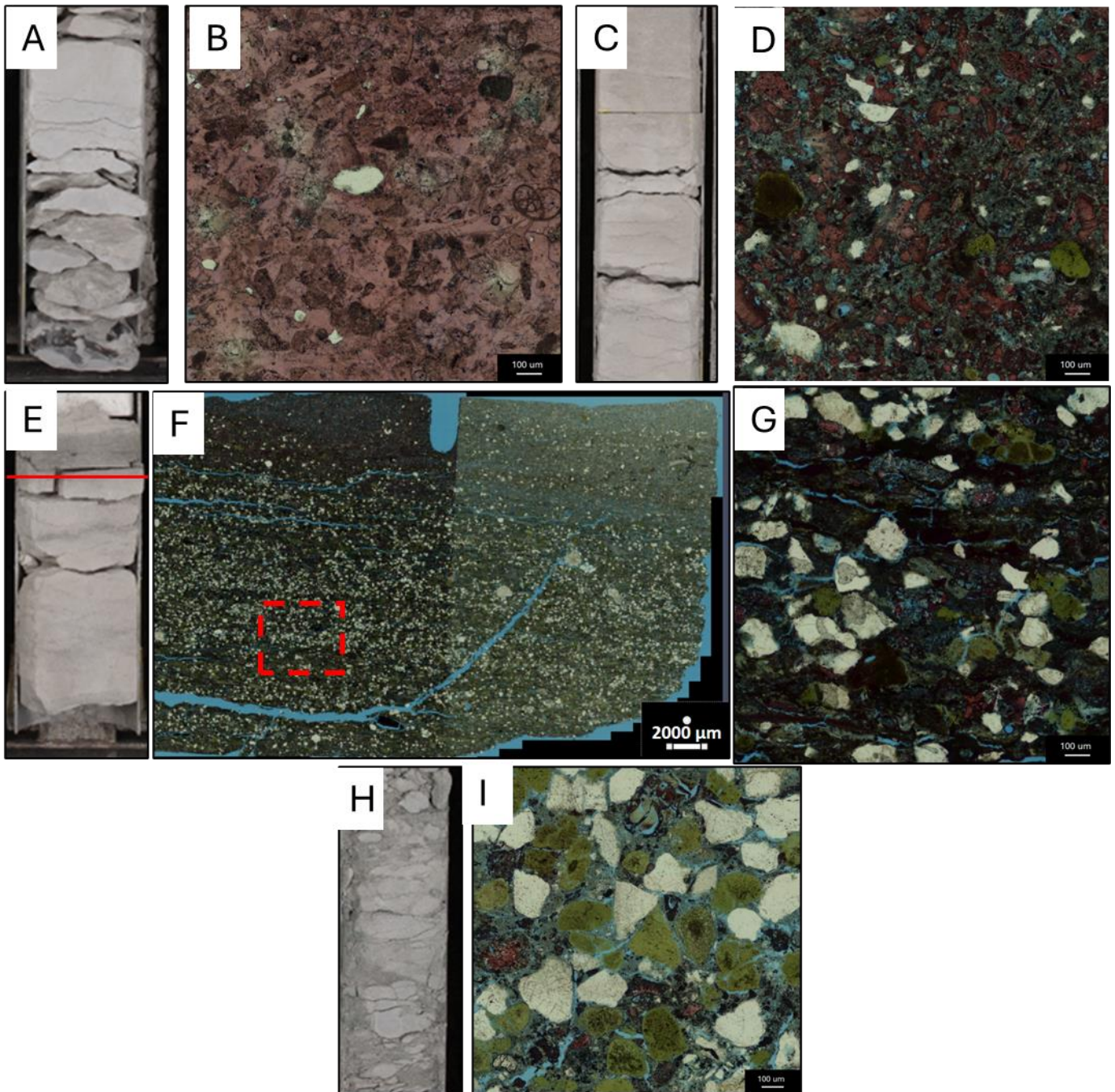


Fig. 8: Facies of the mixed siliciclastic and carbonate interval (Gulpen Fm.) showing bioturbated, bioclastic, glauconitic carbonate rocks (A&C). The siliciclastic dominated beds in the mixed part of the core (E&H). The core photos represent lithofacies. Thin sections photos represent microfacies. **A)** B1 (245.7-245.5 m). **B)** M4 associated with lithofacies B1 TS# B192 – 245.6 m BI=1-4. **C)** B2 (232.7-232.5 m). **D)** M5 associated with lithofacies B2 TS# B160 – 232.6 m BI=2-5. **E)** B3 (243.9-243.7 m) Facies B3 is above the red line. **F)** Zoomed out photo for microfacies M6 showing the laminated quartz layers. M6 is associated with lithofacies B3 TS# B187 – 243.7 m. The red box shows the location of the zoomed in photo in Fig. **G)** Zoomed in photo M6. **H)** B4 (235.2-232.3 m). **I)** M7 associated with lithofacies B4 TS# B166 – 234.9 m.

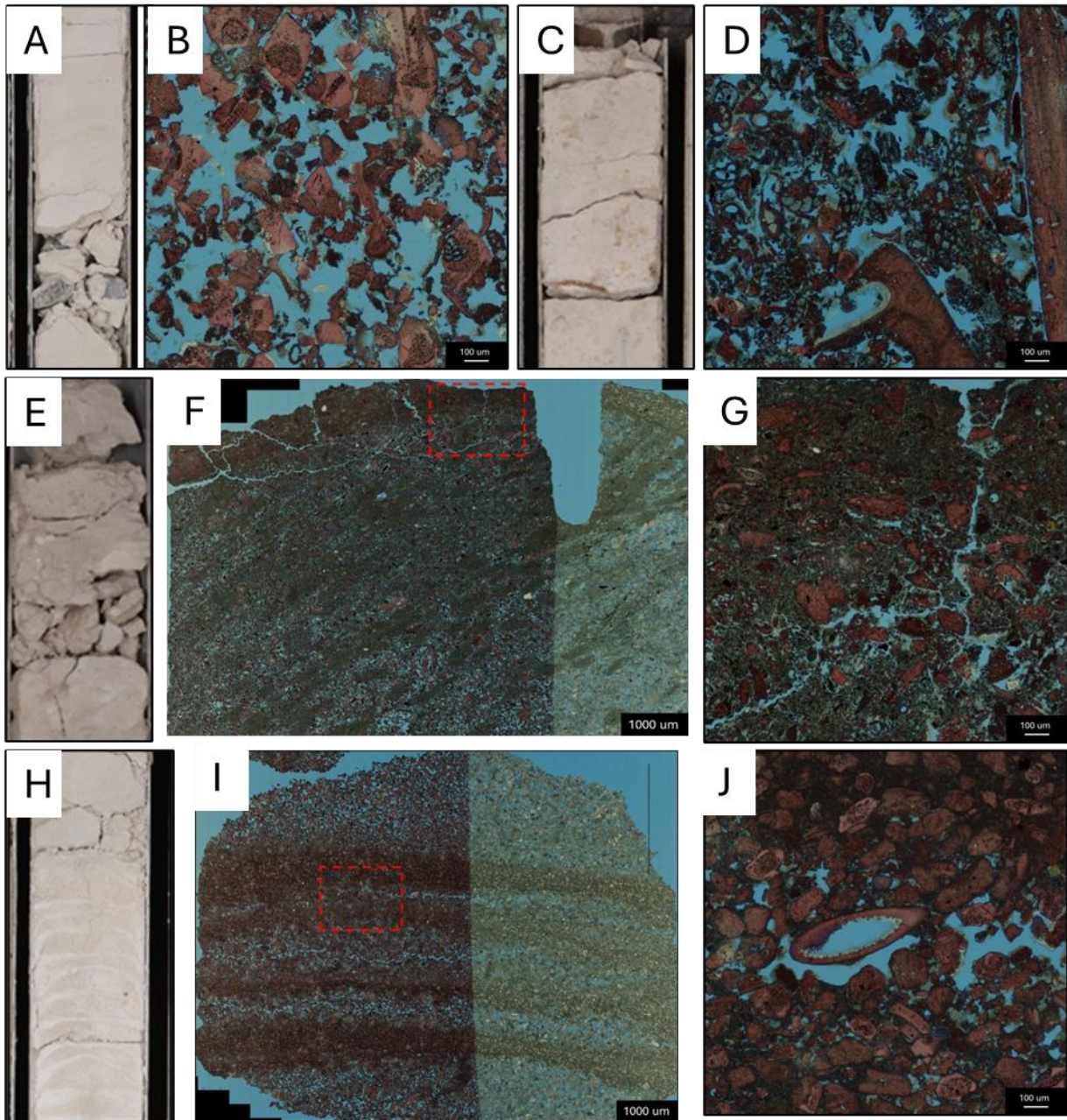


Fig. 9: Facies of the pure carbonate interval (Maastricht Fm.) showing bioturbated, bioclastic, porous carbonate rocks. The core photos represent lithofacies. Thin sections photos represent microfacies units. **A)** C1 (188.6-188.4 m). **B)** M8 associated with lithofacies C1 TS# B54 – 188.5 m. **C)** C2 (175.4-175.1 m). **D)** M9 associated with lithofacies C2 TS# B22 – 175.3 m. **E)** C3 (174.2-174 m) **F)** Zoomed out photo of microfacies M10 showing the laminated muddy layer in the uppermost part of the thin section (BI=5). M10 is associated with lithofacies C3 TS# B19 – 174 m. The red box shows the location of the zoomed in photo in Fig. G. **G)** Zoomed in photo M10. The muddy matrix observed in thin section corresponds with the gamma ray spike in the Maastricht Formation **H)** C4 (169.9-169.7 m) note the presence of drilling induced deformation during the coring job. **I)** Zoomed out photo of microfacies M11 showing the laminations that are induced by the drilling. **J)** Zoomed in photo of M11 associated with lithofacies C4 TS# B10 – 169.9 m. note that in the zoomed in photo no dissolution is observed in the boundary between the “laminated beds” which rules out the idea that beds were compacted and then was subjected to differential dissolution.

3.2 Description of the Eys01 borehole

The core description of the Eys01 borehole from Kooij (2023) is summarized in this section and correlated with the deposits encountered in the Beek04 borehole (Fig. 10). Moreover, observations made on the cores of the Eys01 borehole by Kooij (2023) were used in the discussion section. According to Kooij, (2023) the cored interval (16-111 m) in Eys01 borehole recovered the Vaals Formation, Gulpen Formation and Kunrade facies (in this paper it will be referred to as “Kunrade Formation”) (Fig. 10). The Vaals Formation in Eys01 borehole is made up primarily of siliciclastic material and is approximately 10 meters thick. The cores did not recover the Vaals-Gulpen formations contact, as roughly 35 cm of material was missing from the cores. However, there is a sharp transition observed on the cores from the siliciclastic dominated deposits of the Vaals Formation to the calcareous deposits of the Gulpen Formation. In Eys01 borehole, the Gulpen Formation is mostly composed of light colored, bioturbated, bioclastic siltstones with a larger amount of siliciclastic material observed in the lower and upper parts when compared to the middle part of the formation with common occurrence of flint. The transition between the Gulpen and Kunrade formations is a gradual transition as observed from the data. The overlying Kunrade Formation is made up of bioturbated, silt sized, bioclastic limestones that show alternations of indurated and soft layers. The Eys01 borehole recovered the Kunrade Formation whereas the Beek04 borehole recovered the Maastricht Formation.

Beek04						
Formation	Porosity (%)			Horizontal Permeability (mD)		
	Max.	Min.	Avg.	Max.	Min.	Avg.
Vaals	5%	1%	2%	2800	0.13	176
Gulpen	19%	0%	3%	9100	0.14	194
Maastricht	40%	8%	31%	90700	1.70	18617
Eys01						
Vaals	19%	1%	1%	598	5.60	35
Gulpen	6%	0%	1%	623	0.29	26
Kunrade	5%	0%	2%	315	0.80	18

Table 1: Summary of the porosity and permeability measurements of Beek04 and Eys01 boreholes. Eys01 borehole data are from Kooij (2023).

Approx. 30 Km

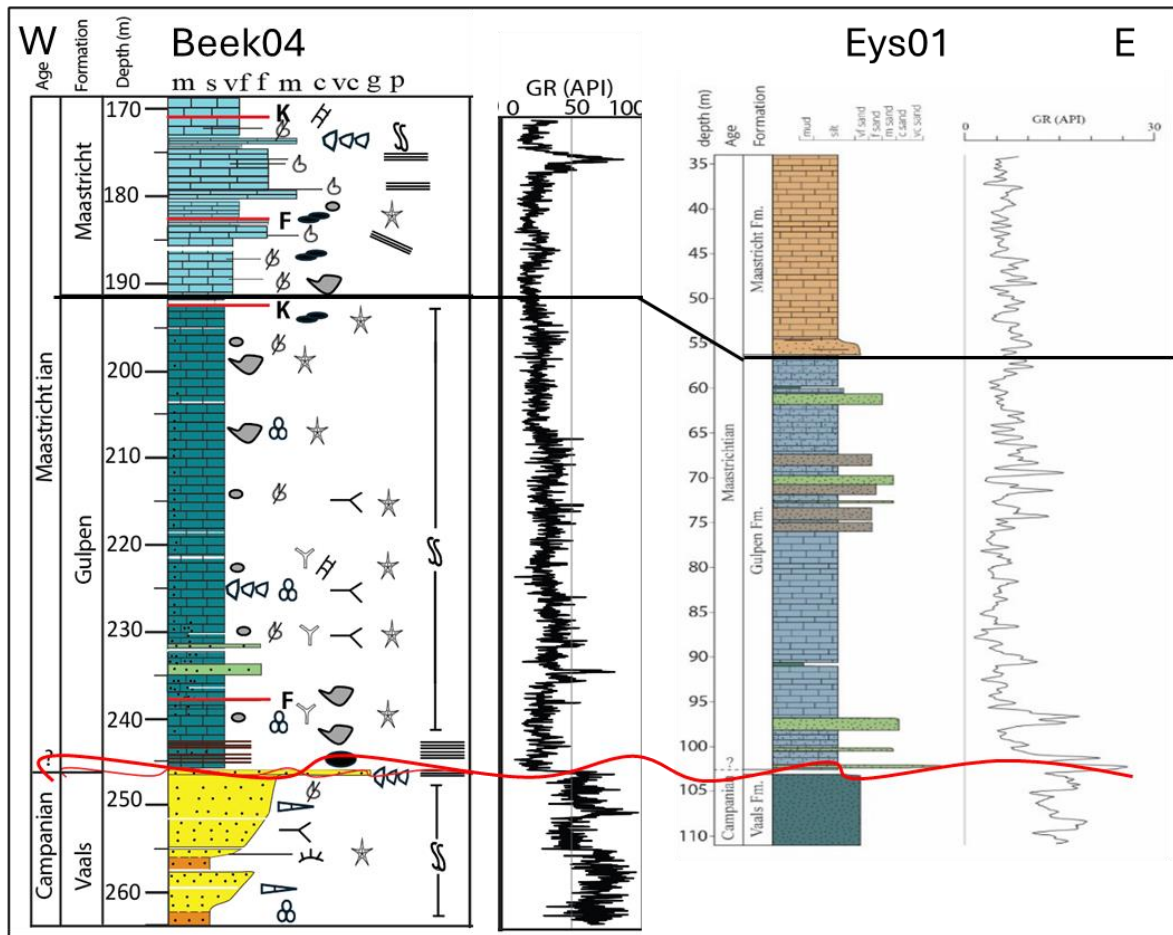


Fig. 10: Correlation panel showing Beek04 in the west of south Limburg with Eys01 in the east. The Eys01 core description and related data were obtained from Kooij (2023). Note the similarities between the Vaals and Gulpen formations in both boreholes in terms of lithology and GR signature. The upper part of the cores shows different characteristics in both boreholes which is related to the recovery of different formations. In the east, Eys01 borehole recovered the Kunrade Formation whereas the Beek04 recovered the Maastricht Formation. Note: GR signatures can be used as a first pass correlation scheme in the region of South Limburg where the boundaries between the formations can be observed.

4. Discussion

4.1 Stratigraphy of Beek04 borehole and South Limburg

In this part of the research, the deposits of the Chalk Group in Beek04 will be assigned to different formations following the lithostratigraphic definitions of Felder (1975) and Felder & Bosch (2000). In addition, the deposits from the Beek04 borehole will be correlated with the deposits from the Eys01 borehole (Kooij, 2023) to investigate the lateral continuity of the Chalk Group formations in South Limburg. Lastly, observations made on both boreholes will be compared with observations made on the rocks of the Chalk Group in South Limburg from previous publications.

4.1.1 Vaals Formation

In Beek04 borehole, the siliciclastic dominated interval in the bottom part of the cores (264 - 246 m) is interpreted to be part of the Vaals Formation (Fig. 4). The observed glauconite bearing siltstones and sandstones in Beek04 borehole are of marine origin as they contain marine fossil fragments such as foraminifera and bivalves (Fig. 7). In South Limburg, the Campanian Vaals Formation is made up of, calcareous, fine grained marine sandstones and coarse siltstones with varying amount of clay and authigenic glauconite present in the rocks (Schmid, 1959; Felder, 1975; Jagt et al., 1987; Bless et al., 1987) which is similar to the deposits found in the Beek04 borehole and the deposits of the Eys01 borehole (Kooij, 2023).

The sediments of the Vaals Formation are bioturbated and contain a varying amount of authigenic glauconite and clay (Fig. 11A&B). Based on that, Albers et al., (1979) suggested that the Vaals Formation was deposited below the fair-weather base. In addition, Zijlstra (1995) suggested that the Vaals Formation was deposited in a shallow marine environment in which glauconite precipitated and then reworked by bioturbation.

The CaCO₃ content of the Vaals Formation in the Campine basin ranges from 2 to 30%, with the greatest values found in the west and northwest. (Felder et al., 2000). In Beek04 borehole, the CaCO₃ content ranges from 10-20% which is higher than the CaCO₃ content observed by Kooij (2023) in the Eys01 borehole (2-10%) which can be indicative of a slight deepening of the depositional environment to the west of South Limburg.

According to Felder (1975) and Zijlstra (1995), at the base of members or cycles in the Vaals Formation cross bedding is commonly observed. However, In the Beek04 borehole that wasn't the case as no sedimentary

structures were observed within the Vaals Formation (Fig. 11C). A Few, thin less than 10 cm of laminated sands were observed in the Eys01 borehole (Kooij, 2023) and are the only sedimentary structure observed within the Vaals Formation in both boreholes. The absence of sedimentary structures in the Vaals Formation in the boreholes can be related to the intense bioturbation of the rocks during deposition. According to Zijlstra (1995), intense bioturbation during deposition of the rocks can destroy any depositional sedimentary structures. During the waning stage of storms, deposition rate is slower than burrowers could rework the sediments, hence sedimentary structures were not preserved (Zijlstra, 1995).

The gamma ray log can be used to differentiate between the Vaals and Gulpen formations in South Limburg. The abrupt change from the siliciclastic dominated Vaals with higher gamma ray signature to a mixed carbonate and siliciclastic Gulpen Formation with a lower gamma ray signature can be clearly observed in both boreholes (Fig. 10).

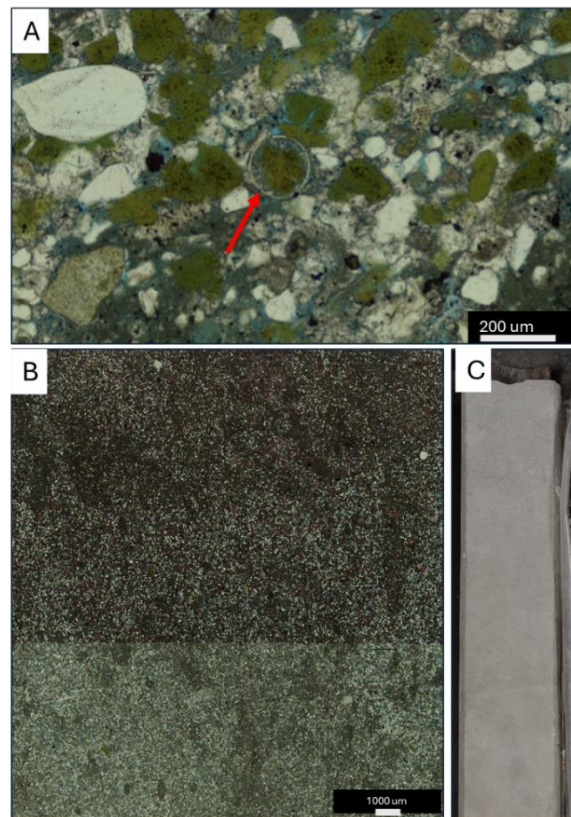


Fig. 11: **A)** The red arrow points to authigenic glauconite growing inside the foraminifera observed in microfacies M2 TS# B218 – 255.1 m. **B)** Microfacies M2 TS# B215 – 253.8 m showing the intense bioturbation of the Vaals Formation (BI:4-5). **C)** Lithofacies A2 258.7-258.2 m showing the absence of sedimentary structures in the Vaals Formation which can be related to the bioturbation and the amount of clay observed in the thin sections.

4.1.2 Gulpen Formation

The current DINOloket DGM model assumes that the Gulpen Formation is entirely missing in the Beek04 borehole (Fig. 3), and the mixed siliciclastic and carbonate interval (246-192 m) encountered in the Beek04 borehole is assumed to be part of the Maastricht Formation. However, the deposits of that interval show better resemblance to the description of the Gulpen Formation in South Limburg of Felder (1975) and Felder & Bosch (2000) (Fig. 4). The Gulpen Formation is composed of soft limestones with chert nodules (Felder & Bosch, 2000; Felder, 1975). According to Felder & Bosch (2000), flint nodules are commonly found at the top of the formation, accounting for around 20% of the volume. In addition, the formation's bottom has a lower carbonate content (50-90%) than the top (85-90%) and contains more glauconite (Felder and Bosch, 2000). Therefore, the mixed siliciclastic and carbonate interval (246-192 m) in the Beek04 borehole is interpreted to be part of the Gulpen Formation not the Maastricht Formation. This marks the first step toward improving the (hydro)stratigraphic model of South Limburg.

The glauconite bearing mixed siliciclastic and carbonate rocks were encountered in the Eys01 borehole and interpreted to be part of the Gulpen Formation as well (Kooij, 2023). Even though those deposits best resemble the Gulpen Formation, they do not match the descriptions of any of the members of the Gulpen Formation as formally defined by Felder & Bosch (2000) (Fig. 12). Kooij (2023), interpreted that the Eys01 borehole recovered the Vijlen member of the Gulpen Formation based on the expression of glauconite in the rocks which is similar to the description of Keutgen et al., (2010) for the Vijlen member of the Gulpen Formation in South Limburg. Even though the glauconite expression is also similar in the Beek04 borehole (Fig. 13), the lithology of the Vijlen member is different than the lithology of the deposits found in both boreholes. According to Albers (1979) and Felder (1997), the Vijlen member is laterally heterogeneous and relatively purer in terms of carbonate content in the west of the Campine basin (95%) when compared to the eastern part (50-80%). However, the recovered Gulpen Formation shows siliciclastic beds and laminated intervals in both boreholes. Such laminations were not mentioned or observed in the literature of the region of South Limburg. The Eys01 and Beek04 boreholes recovered two distinct siliciclastic beds in the Gulpen Formation: poorly sorted greensands and quartz, and glauconite-rich sandstones. Despite having a similar composition, these beds differ in texture. The literature does not distinguish between these types of siliciclastic beds, and the latter bed has not been described previously.

Based on that, both Beek04 and Eys01 boreholes recovered the “pre-Valkenburg strata” of the Gulpen Formation which best matches the description of the deposits encountered in the cores. According to Felder

(1985), the “pre-Valkenburg strata” are transitional facies found in between the Vaals and Maastricht formations forming the lateral equivalent to the Gulpen Formation in South Limburg. In addition, it was observed near areas that are affected by faults, which is the case in both boreholes (Fig. 1). According to Jagt et al., (1987), it is made up of quartz rich, glauconite bearing limestones and contains erosional products associated with the Roer Valley Graben inversion. This can explain the higher siliciclastic content observed in both boreholes when compared to the siliciclastic content of the Gulpen Formation in the region

According to Zijlstra (1995) glauconite replaced carbonate clasts and was precipitated in the pore spaces, indicating that glauconite is an authigenic mineral. Similar to the observations made on the cores of the Beek04 borehole, glauconite at the base of the Gulpen Formation is high in concentration when compared to the top. A decrease in the amount of glauconite as we move up the stratigraphy indicates that the glauconite was eroded and then redeposited (Zijlstra, 1995).

Flint concentrations are commonly found in the Gulpen and Maastricht formations. According to Bischoff and Sayles (1972) and Zijlstra (1995), precipitation zones can be found near burrows and their orientation is parallel to the seabed. The growth of flint nodules is inversely proportional to the sedimentation rate. In order to form nodular flint layers, sedimentation rate needs to be low and almost zero (Zijlstra, 1995).

Flint concretions observed in the lower part of the Gulpen Formation in Beek04 and Eys01 (Kooij, 2023) boreholes start as black, tabular and extensive layers with burrows (Fig. 14A). As we move up the stratigraphy, two modes of flint occurrence were observed. The first one is light grey and weakly developed flint nodules, which is the most common occurrence (Fig. 14C). The second one is dark grey, weakly developed concretions, slightly extensive and patchy (Fig. 14B). Flint formation in the Beek04 and Eys01 borehole can be indicative of sedimentation rate. The most well-developed flint concretions are located at the bottom of the Gulpen Formation which indicates lower sedimentation rates at the start of the Gulpen deposition when compared to the middle part which contains the weakest developed concretions which are indicative of a higher sedimentation rate. Towards the top of the Gulpen formation, flint nodules increase in size and concentration. Thus, an alternation between higher and lower energy conditions as well as sedimentation rates can be inferred from the flint mode.

Age		Member	Horizon	General Description
Late Cretaceous	Maastrichtian	Lanaye	Nivelle	White, fine grained limestones with light to dark grey flint nodules
		Lixhe 3	Boirs	White to light grey, very fine grained limestone with dark flint concretions
		Lixhe 2	Halembaye 1	
		Lixhe 1	Wahlwiller	
	Campanian	Vijlen	Bovenste Bosch	Light grey, fine grained, glauconitic limestones
		Beutenaken	Sienaken	Fine to coarse sandstone with limestone nodules
		Zeven Wagen	Zeven Wagen	White chalk

Fig. 12: Subdivision of the Gulpen Formation after Felder & Bosch (2000). Note that the horizons occur at the base of the corresponding member.

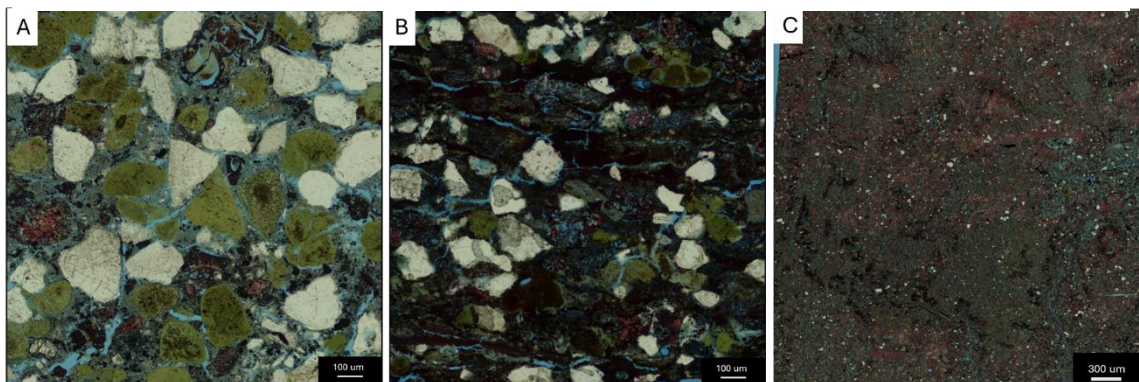


Fig. 13: In the Beek04 borehole, glauconite is present in the Gulpen Formation in three different modes. The first mode is within the rock fabric, the second mode is associated with bioturbation as a burrow infill and the third mode can be associated with quartz grains and deposited in different layers

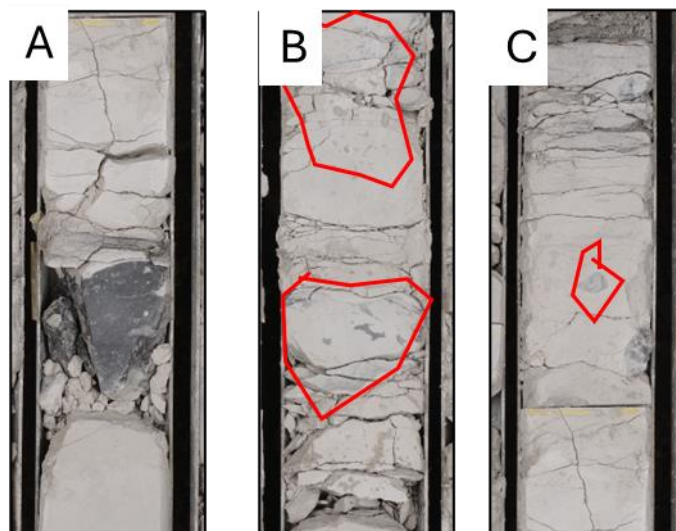


Fig. 14: Flint nodules observed in the Gulpen Formation in Beek04 borehole. **A)** Black, tabular and extensive layers 245.5 m. **B)** Grey, irregular, slightly extensive and weakly developed concretions 203.2 m. **C)** light grey, weakly developed flint nodules 245.6 m.

4.1.3 Maastricht Formation

In the Beek04 borehole, the interval between (192-167 m) (Fig. 4) is interpreted to be part of the Maastricht Formation. In South Limburg, the Maastricht Formation is generally composed of soft, fine to coarse-grained limestones (Felder & Bosch, 2000). According to Felder & Bosch (2000) and Felder (1975) the formation can be subdivided into lower and upper parts. The lower part is made up of fine-grained limestones with 5-12% flint content, while the upper part is fine to very coarse-grained limestones with almost no flint content <1% and contains very coarse grained 20-50 cm thick fossil layers every 1-5 m interval.

Four coarser fossil layers were observed in the cores of the Beek04 borehole (Fig. 4) but not in Eys01 borehole (Kooij, 2023). The thickness of the fossil layers is 1-20 cm (Fig. 15B). Two of which were serpulid layers (Fig. 15C). Serpulids indicate a shallow and warm environment with a solid substrate (Felder, 2001). In addition, an increase in the grain size from very fine to fine was observed at approximately 190 m represented by lithofacies unit C2. The presence of coarse fossil layers accompanied by an increase in grain size can be indicative of an increase in hydrodynamic conditions. According to Zijlstra (1995), fossil clasts with larger grain sizes imply higher energy conditions, which can be related to shallower depositional environments or increased storm intensity (Zijlstra, 1995).

In Beek04 borehole, I observed the presence of cross bedding within the Maastricht Formation (Fig. 15A). However, that was not the case in Eys01 borehole as no cross bedding was observed in the Kunrade Formation (Kooij, 2023). According to descriptions from Zijlstra (1995), cross bedding was observed in the Maastricht Formation as well.

In addition to the differences mentioned above between the Maastricht Formation in the Beek04 borehole and the Kunrade Formation in the Eys01 borehole (Fig. 16 A&B). In the Beek04 borehole, I observed very fine-grained limestones with low chert content at the bottom of the Formation and medium to coarse grained limestone with no chert content and coarse fossil layers in the upper part. In contrast, the Kunrade Formation in the Eys01 borehole is made up of highly bioturbated, yellowish bioclastic silt sized carbonate rocks with alternation of cemented and non-cemented layers mixed with siliciclastic material (Kooij, 2023). Also, enriched glauconite pellet layers of approximately 1 m thickness are observed at the base of the Kunrade Formation in the Eys01 (Kooij, 2023) but not in the Beek04.

The differences discussed above in the recovered Maastricht and Kunrade formations when comparing both boreholes can testify to the heterogeneity of the Chalk Group formations in South Limburg. In addition, it supports the findings of Kroth et al., (2024) which suggests that the Kunrade facies should be given the status of formation as it is mappable in the eastern part

of South Limburg, and it show significant differences than the Maastricht facies. Thus, Felder & Bosch (2000) subdivision of the Maastricht Formation into two informal units, Maastricht facies in the west and Kunrade facies in the east of South Limburg is less feasible. Moreover, the differences observed are also related to aquifer properties which are important to the region of South Limburg. The Maastricht Formation encountered in the Beek04 borehole shows extremely high porosity and permeability values when compared to the Kunrade Formation encountered in the Eys01 borehole which is related to cementation (Fig.16 A&B) (Table 1). This is important when investigating the lateral continuity of the Chalk Group formations in South Limburg and can be used as an input to improve the current (hydro)stratigraphic model of South Limburg.

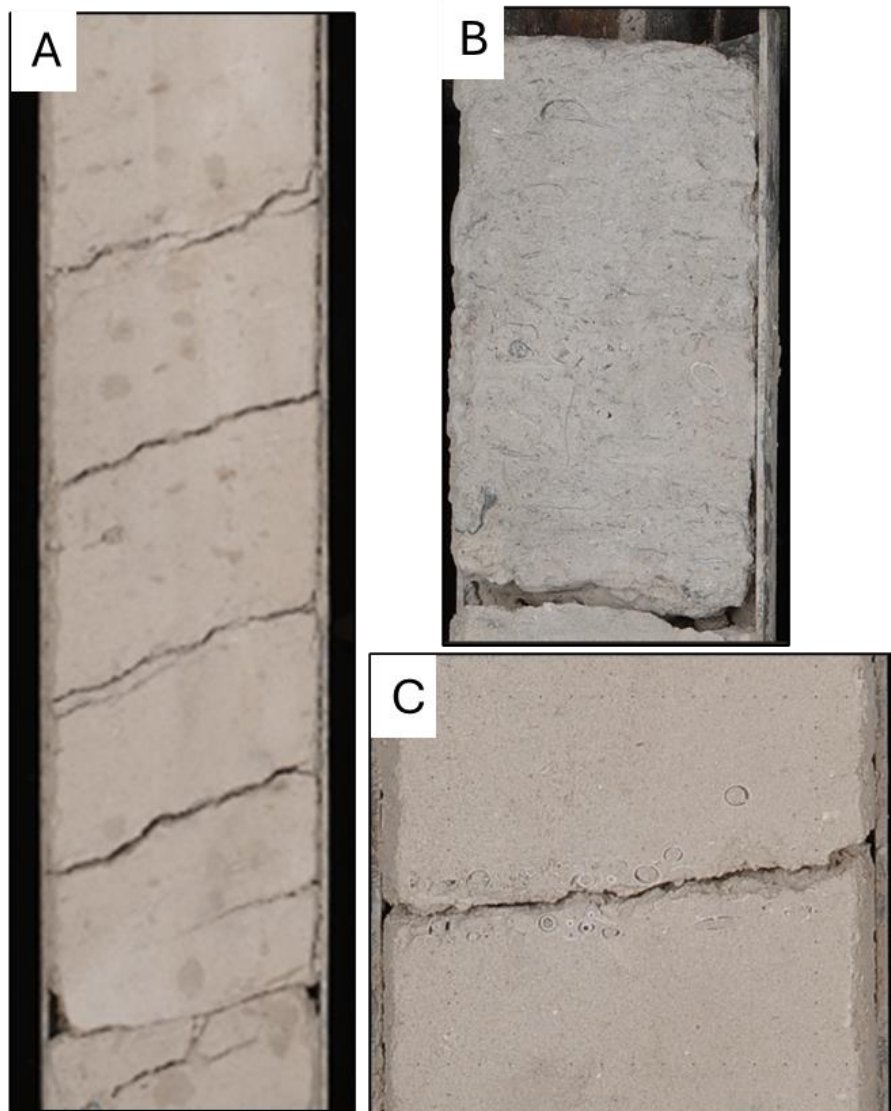


Fig. 15: **A)** Cross bedding observed in the Maastricht Formation lithofacies C2 176.8 - 176.5 m. **B)** Fossil layer encountered in the Maastricht Formation lithofacies C2 (180.5-180.3 m). **C)** Serpulide layer in the Maastricht Formation lithofacies C2 at 176.3 m.

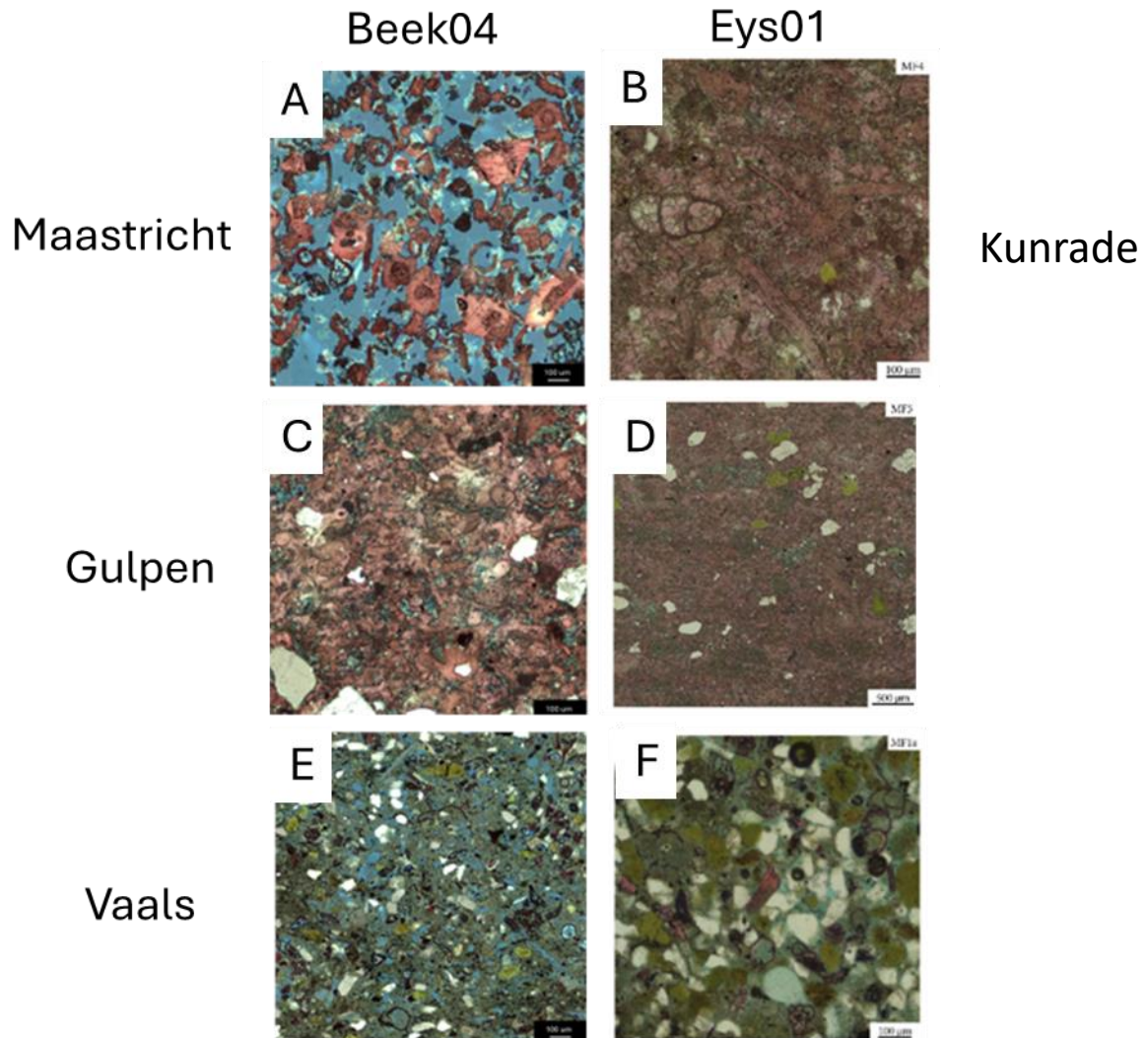


Fig. 16: Comparing thin sections from Beek04 and Eys01 boreholes taken from Vaals, Gulpen, Maastricht and Kunrade formations. **A&B)** The Maastricht and Kunrade formations show different characteristics in both boreholes. The main difference between the two is in the Beek04 we notice the syntaxial calcite cement growing around the bioclasts while in the Eys01 we notice blocky calcite cementation replacing the matrix, bioclasts and plugging both porosity and permeability. **C&D)** Shows the similarities between the Gulpen Formation in both boreholes represented by mixed carbonate and siliciclastic deposits that are calcite cemented with rare quartz and glauconite content. **E&F)** highlighting the similarities in Vaals Formation. In both boreholes the Vaals Formation is composed of bioturbated, bioclastic, glauconitic sandstones.

4.2 Roer Valley Graben Inversion Influence on South Limburg

The data from Beek04 borehole can be used to shed light on the influence of the Roer Valley Graben inversion to the region of South Limburg in order to understand the heterogeneities of the formations of the Chalk Group. In the literature, scientists argue that the inversion began during Campanian associated with the Vaals Formation deposition (Kuyl, 1983; Bless et al., 1987), while others suggest that it began earlier in the Cenomanian (Gras, 1995). The Beek04 borehole did not recover the Cenomanian succession but, it recovered the upper part of the Vaals Formation which is of Campanian to Late Campanian age. Therefore, the Beek04 borehole data is limited to study the inversion's influence on the geology of the region.

According to Gras & Geluk, (1999), the inversion led to the deposition of the Vaals Formation in South Limburg. The deposition of the Vaals Formation is considered homogenous and is characterized by glauconite bearing sandstones and siltstones (Felder, 1985).

The upper part of the Vaals Formation and the contact with the overlying Gulpen Formation in the Beek04 borehole are shown in (Fig. 5). The difference in size and roundness of the quartz grains of microfacies M3 (Fig. 5B) can be indicative of mixed sediment sourcing, or the coarser grains can be related to the inversion, uplifting and redepositing older deposits with Upper Cretaceous rocks. In addition, microfacies M3 is overlain by lithofacies A3 (Fig. 5A) that is characterized as a breccia, where laminated fragments of the same rock were eroded and redeposited in different orientations (Fig. 7E). Both facies can be related to inversion tectonics that affected the region in the Late Campanian.

The contact between the Vaals Formation and the overlying Gulpen Formation is interpreted to be an unconformity surface where parts of the Gulpen Formation are missing, and the Vaals Formation is overlain by the "pre-Valkenburg strata" of the Gulpen Formation. According to Felder (1985), the presence of sedimentary gaps between the Vaals and the Gulpen formations must be accepted in the region of South Limburg. In addition, in Northwest Europe, Huigen (2014), Saes (2013), and Anderskov and Surlyk (2011) identified a widespread erosional unconformity of Late Campanian age in the Netherlands, Germany, the United Kingdom, Norway and Denmark that is related to the sub-hercynian inversion phase.

The Gulpen Formation in the Beek04 and Eys01 boreholes is characterized by a higher siliciclastic content with siliciclastic dominated facies when compared to the formal definition of the Formation by Felder & Bosch (2000). Most of the studies on the Gulpen Formation were done in the southern part of South Limburg where the formation is exposed (e.g., the ENCI and Hallembaye quarries). The Gulpen Formation in the Southern part is mainly composed of finer grained chalk deposits with minor

siliciclastic material (Vellekoop et al., 2022). The higher siliciclastic content of the Gulpen Formation in the north part of South Limburg can be interpreted as an effect of the Roer Valley Graben inversion, where areas proximal to the inverted graben received more erosional products. According to Bless (1988), the Roer Valley Graben may have been an island or shoal when siliciclastic debris was transported into deeper settings during high energy spring tides and storms.

The general decrease in the siliciclastic content of the Gulpen Formation as we move up the stratigraphy in the Beek04 borehole is consistent with the findings of Bless et al., (1987) where they suggest that the Roer Valley Graben was flooded due to continuous sea level rise. Thus, less siliciclastic material was transported into the basin. In addition, the Maastricht Formation in the Beek04 borehole is composed of pure carbonates and the contact between the two formations is gradual. This is consistent with the interpretations of Gras and Geluk (1999), which suggest that the Roer Valley Graben was flooded completely during the Late Maastrichtian due to subsidence. Thus, almost no siliciclastic material was observed in the Maastricht Formation in the Beek04 borehole. In contrast, the Kunrade Formation in the Eys01 borehole contains siliciclastic material. However, the presence of siliciclastic material in the Kunrade Formation can be explained by the findings of Kroth et al., (2024), suggesting that the eastern part of South Limburg is more proximal in terms of depositional setting when compared to the western part.

Finally, the inversion effects were observed at the contact between the Vaals and Gulpen formations in the Beek04 borehole. After that, the influence of the inversion is decreasing over time as less siliciclastic material was supplied to the basin from the inverted Roer Valley Graben. Therefore, based on the data from the Beek04 borehole, the inversion influence was highest at the contact between the Vaals and Gulpen formations. Similar to interpretations made by Gras (1995) and Gras & Geluk (1999) proposing that the Gulpen and Maastricht formations were deposited after the inversion. However, some writers suggested that the inversion of the Roer Valley Graben ended at the boundary between the Gulpen and Maastricht formations (Kuyl, 1983; Bless, 1988, 1989). This is unlikely as the contact between the two formations is gradual in both the Beek04 and Eys01 boreholes.

5. Conclusions

- The deposition of the Chalk Group in South Limburg can be subdivided into three stages, siliciclastic dominated deposits, followed by mixed siliciclastic and carbonate deposits, and finally, pure carbonate deposits.
- The findings of this study suggest that the cored interval in Beek04 borehole (246-191.5 m) is part of the Gulpen Formation not the Maastricht Formation as currently stated in the DGM model of DINOloket.
- The contact between the Vaals and the Gulpen formations in Beek04 and Eys01 boreholes is unconformable where the Vaals Formation is overlain by the pre Valkenburg strata of the Gulpen Formation.
- Beek04 borehole recovered the pre Valkenburg strata of the Gulpen Formation that is characterized by a high siliciclastic content.
- The siliciclastic material in the Gulpen Formation were most likely sourced from the erosional products of the inverted Roer Valley Graben and transported during high energy events.
- The contact between the Gulpen and Maastricht formations in Beek04 borehole is characterized by a general decrease in the siliciclastic and glauconite content of the carbonate rocks gradually over approximately 14 m (206-192).
- The findings from this study support the subdivision of the Maastricht Formation in South Limburg into two formations. Kunrade Formation located in the eastern part (Eys01) and Maastricht Formation located in the western part (Beek04) of South Limburg.
- The Maastricht Formation in the Beek04 borehole is characterized by extremely high porosity and permeability and corresponds to the best aquifer of the Chalk Group in South Limburg.
- Gamma ray log can be used to aid in the correlation of the Chalk Group in South Limburg. The Vaals Formation can be distinguished from both Gulpen and Maastricht formations due to its higher gamma ray signature. Gulpen Formation displays a more spikey and slightly higher gamma ray signature due to the higher siliciclastic content of the rocks when compared to the Maastricht Formation.

References:

- Albers, H.J.**, (1974). Feinstratigraphie und faziesanalyse des Untercampanans (Vaalser Grünsand) sowie neue Beiträge zur kretazischen Deckgebirgstektonik von Aachen und dem westlich anschliessenden niederländisch-belgischen Limburg. Diss., Fak. Bergbau und Hüttenkunde, Geol. Inst. Der RWTH, Aachen.
- Albers, H.J., Felder, W.M.**, (1979). Litho-, Biostratigraphie und Palökologie der Oberkreide und des Alttertiärs (Präobersanton-Dan/Paläozän) von Aachen-Südlimburg. Aspekte der Kreide Europas. IUGS Series A, nr. 6, p. 47 – 84.
- Anderskov, K., Surlyk, F.**, (2011). Upper Cretaceous chalk facies and depositional history recorded in the Mona-1 core, Mona Ridge, Danish North Sea. Geol. Surv. Den. Greenl. Bull. 25, pp. 1-60.
- Baldschuhn, R., Best, G. and Kockel, F.** (1991). Inversion tectonics in the Northwest German Basin. In: Spencer, A.M. (ed.): Generation, accumulation, and production of Europe's hydrocarbons Special Publication, European Association Petroleum Geoscientists. Oxford University Press (Oxford) 1: 145–159.
- Bischoff, J.L., Sayles, F.L.**, (1972). Pore fluid and mineralogical studies of recent marine sediments. J. Sedim. Petrol., 41, p. 711-724.
- Bless, M.J.M.** (1988) Upper Campanian lithofacies and ostracode assemblages in South Limburg and NE Belgium. In: The Chalk District of the Euregio Meuse-Rhine. Selected papers on Upper Cretaceous deposits, 57–67.
- Bless, M.J.M., Felder, P.J., Meessen, J.P.M.T.**, (1987). Late Cretaceous sea level rise and inversion: their influence on the depositional environment between Aachen and Antwerp. Ann. Soc. Géol. Belg., 109, 2, p. 333-355.
- Bless, M.J.M.**, (1989). Event-induced changes in Late Cretaceous to Early Paleocene ostracode assemblages of the SE Netherlands and NE Belgium. Ann. Soc. Geol. Belg., 112 (1), p. 19-30.
- Bromley, R.G.**, (1975). Trace fossils at omission surfaces. In: The study of Trace Fossils. SpringerVerlag New York Inc., p. 399-428.
- Bostyn, Françoise, Jacek Lech, Alan Saville, and Dagmara H. Werra.** (2023) Prehistoric Flint mines in Europe. Oxford, -: Archaeopress Archaeology.

- Burst, F.J.**, (1958). ‘‘Glaucinite’’ pellets: their mineral nature and applications to stratigraphic interpretations. *Bull. Amer. Assoc. Petrol. Geol.*, 39, p. 484-492.
- Campbell, C.V.** (1967) Lamina, Laminaset, Bed and Bedset. *Sedimentology*, 8(1), 7–26. <https://doi.org/10.1111/j.1365-3091.1967.tb01301.x>.
- Choquette, P.W. and Pray, L.C.** (1970) Geologic nomenclature and classification of porosity in sedimentary carbonates. *AAPG bulletin*, 54, 207–250. Choquette, P.W. and Pray, L.C. (1970) Geologic nomenclature and classification of porosity in sedimentary carbonates. *AAPG bulletin*, 54, 207–250.
- Cloetingh, S.**, (1986). Intraplate stresses: a new tectonic mechanism for fluctuations of relative sea level. *Geology* 14: 617–620.
- Crittenden, S.**, (1987). The ‘Albian transgression’ in the southern North Sea Basin. *Journal of Petroleum Geology* 19: 395–414.
- Droser, M. L., and D. J. Bottjer.** (1986) ‘‘A Semiquantitative Field Classification of Ichnofabric.’’ *Journal of Sedimentary Research* 56, no. 4 (July 1, 1986): 558–59. <https://doi.org/10.1306/212f89c2-2b24-11d7-8648000102c1865d>.
- Dumont, A.H.**, (1849). Rapport sur la carte géologique du Royaume. –*Bull. Acad. Roy. Sci. Lett., Beau-Arts Belgique*, XVI (11), p. 351-373.
- Dunham, R.J.** (1962) Classification of Carbonate Rocks According to Depositional Texture, 108–121.
- Felder, P.J., Bless, M.J.M., Demyttenaere, R., Duser, M., Meessen, J.P. M.T. & Robaszynski, F.**, (1985). Upper Cretaceous to Early Tertiary deposits (Santonian-Paleocene) in northeastern Belgium and South Limburg (The Netherlands) with reference to the Campanian-Maastrichtian. *In: Belgische Geologische Dienst, Professional Paper* 1985/1. vol. 214, p. 1–151
- Felder, P.J.**, (2001). Bioklasten-stratigrafie of ecozonatie voor het krijt (Santoniaan – Campaniaan – Maasrichtiaan) van Zuid-Limburg en oostelijk België. *Memoirs of the Geological Survey of Belgium* nr. 47.
- Felder, P.S.** (1997) The Vijlen Chalk Member (Maastrichtian, Late Cretaceous) in the Meuse-Rhine Euregion. *Ann. Soc. géol. Belg.*, 119: 119-133.







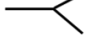











- Felder, W.M.**, (1973), Kalkstenen van het Bovenkrijt in Zuid-Limburg en hun exploitatie. *Verhandelingen koninklijk Nederlands Geologisch mijnbouwkundig Genootschap*, 29, p. 51-62
- Felder, W.M.**, (1975). Lithostratigraphische gliederung der Oberen Kreide. *Publicaties van het Natuurhistorisch Genootschap in Limburg*, aflevering 3 en 4.
- Felder, W.M.** and **Bosch, P.W.**, (2000). Krijt van Zuid-Limburg. *Geologie van Nederland 5*. Nederlands Instituut oor Toegepaste Geowetenschappen TNO (Delft/Utrecht): 190 pp.
- Fitton, W.H.**, (1834). Observation on part of the low Countries and the north of France, principally near Maestricht and Aix la Chapelle. *Proc. Geol. Soc. London*, 14: 161-164.
- Geluk, M.C., Duin, E.J.Th., Duser, M., Rijkers, R.H.B., Van den Berg, M.W.** and **Van Rooijen, P.**, (1994). Stratigraphy and tectonics of the Roer Valley Graben. *Geologie en Mijnbouw* 73: 129–141.
- Gras, R.** (1995) Late Cretaceous sedimentation and tectonic inversion, southern Netherlands. *Geologie en Mijnbouw*, 74, 117–127.
- Gras, R.** and **Geluk, M.C.**, (1999). Late Cretaceous Early Tertiary sedimentation and tectonic inversion in the southern Netherlands. *Geologie en Mijnbouw* 78: 1–19.
- Herngreen, G.F.W., Eillebrecht, A.T.J.M., Gortemaker, R.E., Remmelts, G., Schuurman, H.A.H.M.** and **Verbeek, J.W.**, (1996). Upper Cretaceous Chalk Group stratigraphy near the isle of Texel, the Netherlands (a multidisciplinary approach). *Mededelingen van de Rijks Geologische Dienst* 56: 1–63.
- Herngreen, G.**, and **Wong, T.** (2007). Cretaceous, in geology of the Netherlands. ResearchGate.
- Huijgen, M.**, (2014). Indications for intra-Chalk seals in the F-blocks of the Dutch offshore. MSc Thesis, VU University Amsterdam, 89 p.
- Hofker, J.**, (1966). Maestrichtian, Danian and Paleocene foraminifera. *Palaeontographica*, suppl. 10 (1- 2): 1-376.
- Inden, R.F., Moore, C.H.**, (1983). Chapter 5, Beach Environment. In: Scholle, P.A., Bebout, D.G., Moore, C.H., Carbonate depositional environments. The America Association of Petroleum Geologists Memoirs, nr. 33.

- Jäger, M.**, (1987). Campanian-Maastrichtian Serpulids from Thermae 2000 borehole (Valkenburg a/d Geul, the Netherlands. *Annales de la Société Géologique de Belgique*, 110, p. 39-46.
- Jagt, J.W.M., Felder, P.J., Meessen, J.P.M.T.**, (1987). Het Boven-Campanien in Zuid-Limburg (Nederland) en Noordoost België. *Natuurhistorisch Maandblad*, 76 (4), p. 94-110.
- Jeletsky, J.A.**, (1951). Die Stratigraphie und Belemniten-Fauna des Obercampan und Maastricht Westfalens, Nordwestdeutschlands und Dänemarks sowie einige allgemeine Gliederungs-Probleme der jüngeren borealen Oberkreide Eurasiens. *Geol. Jahrb., Beih.*, 1
- Keutgen, N., Jagt, J.W.M., Felder, P.J. and Jagt-Yazykova, E.A.** (2010) Stratigraphy of the upper Vijlen Member (Gulpen Formation; Maastrichtian) in northeast Belgium, the southeast Netherlands and the Aachen area (Germany), with special reference to belemnitellid cephalopods. *Netherlands Journal of Geosciences*, 89, 109–136.
- Kockel, F.**, (2003). Inversion structures in Central Europe Expressions and reasons, an open discussion. *Netherlands Journal of Geosciences / Geologie en Mijnbouw* 82: 351–366.
- Kooij, R.**, (2023). Facies characterisation of the Gulpen and Maastricht formations (late Campanian–early Danian) in the Eys01 borehole, South Limburg, the Netherlands. MSc Thesis, Utrecht University.
- Kroth, M., Trabuco-Alexandre, J. P., Pimenta, M. P., Vis, G.-J., & De Boever, E.** (2024). Facies characterisation and stratigraphy of the upper Maastrichtian to lower Danian Maastricht Formation, South Limburg, the Netherlands. *Netherlands Journal of Geosciences*, 103, e13. doi:10.1017/njg.2024.9
- Kuyl, O.S.**, (1980). Toelichtingen bij de Geologische Kaart van Nederland 1:50.000, Blad Heerlen. RGD, Haarlem.
- Liebau, A.**, (1978). Paläobathymetrische und paläoklimatische Veränderungen im Mikrofaunenbild der Maastrichter Tuffkreide. – *Neues Jahrbuch für Geologie und Paläontologie*, 157, p. 233-237.
- Lucia, F. J.** (1995). Rock-Fabric/Petrophysical classification of carbonate pore space for reservoir characterization. *AAPG Bulletin*, 79.
- Macquaker, J. H.S., and A.E. Adams.** (2003) “Maximizing Information from Fine-Grained Sedimentary Rocks: An Inclusive Nomenclature for Mudstones.” *Journal of Sedimentary Research* 73, no. 5 (September 1, 2003): 735–44. <https://doi.org/10.1306/012203730735>.

- Megson, J. and Tygesen, T.** (2005) 'The North Sea Chalk: An underexplored and underdeveloped play', *Geological Society, London, Petroleum Geology Conference Series*, 6(1), pp. 159–168. doi:10.1144/0060159.
- Mortimore, R. N.** (2018). Late Cretaceous tectono-sedimentary events in NW Europe. *Proceedings of the Geologists' Association*, 129(3), 392–420.
- Nalpas, Th., Richert, J.-P., Brun, J.-P., Mulder, Th. and Unternehr, P.**, (1996). Inversion du 'Broad Fourteens Basin' ou Graben de La Haye (Sud de la mer du Nord) apports de la sismique 3D. *Bulletin des Centres de la Recherche Exploration-Production, Elf Aquitaine* 20: 309–321.
- Pollock, R.E.** (1976) The depositional environments of the Maastricht and Kunrade Chalks (Maastrichtian) from the type area of Limburg, Netherlands. *Staringia*, 3, 16–18.
- Robaszynski, F., Bless, M.J.M., Felder, P.J., Foucher, J.C., Legoux, O., Manivit, H., Meessen, J.P.M., and van der Tuuk, L.A.**, (1985). The Campanian-Maastrichtian boundary in the chalky facies close to the type-Maastrichtian area. *Bull. Centres Rech. Explor. Prod. Elf-Aquitaine*, 9(1): 1-113.
- Saes, M.**, (2013). An evaluation of the distribution of the Upper Cretaceous Chalk Group in the Dutch Central Graben. MSc. thesis, Utrecht University, 47 p.
- Schiøler, P., Brinkhuis, H., Roncaglia, L. and Wilson, G.J.**, (1997). Dinoflagellate biostratigraphy and sequence stratigraphy of the Type Maastrichtian (Upper Cretaceous), ENCI Quarry, The Netherlands. *Marine Micropaleontology* 31: 65–95.
- Schmid, F.**, (1959). Biostratigraphie du Campanien-Maastrichtien du NE de la Belgique sur la base des Belemnites. *Ann. Soc. Geol. Belg.*, 82: 235-256.
- Uhlenbroek, G.D.**, (1912). Het Krijt van Zuid-Limburg. Jaarverslag Rijksopsp. Delfstof. Over 1911; Den Haag, p: 48-56.
- Van Maanen, J., De Vaan, M. a. J., Veldstra, A. W. F., and Hendrix, W.** (2001). Pesticides and nitrate in groundwater and rainwater in the province of Limburg, The Netherlands. *Environmental Monitoring and Assessment*, 72(1), 95–114. <https://doi.org/10.1023/a:1011963922054>

- Van Wijhe, D.H.**, (1987a). Structural evolution of inverted basins in the Dutch offshore. *Tectonophysics* 137: 171–219.
- Van Wijhe, D.H.**, (1987b). The structural evolution of the Broad Fourteens Basin. In: Brooks, J. & Glennie, K.W. (eds): *Petroleum Geology of North-West Europe*. Graham & Trotman (London): 315–323.
- Vellekoop, J., Kaskes, P., Sinnesael, M., Huygh, J., Déhais, T., Jagt, J. W.M., Speijer, R.P. & Claeys, P.**, 2022. A new age model and chemostratigraphic framework for the Maastrichtian type area (southeastern Netherlands, northeastern Belgium). *Newsletters on Stratigraphy* 55(4): 479–501
- Villain, J.F.**, (1977). Le Maastrichtien dans sa régiontype (Limbourg, Pays-Bas). Étude stratigraphique et micropaléontologique. *Palaeontographica*, A157, p. 1-87.
- Wentworth, C.K.** (1922) A Scale of Grade and Class Terms for Clastic Sediments. *Journal of Geology*, 30, 377-392.
- Zagwijn, W.H. & van Staalduinen, C.J.** (1975) Toelichting geologische overzichtskaarten van Nederland.
- Ziegler, P.A.**, (1982). *Geological Atlas of Western and Central Europe*. Shell Internationale Petroleum Maatschappij B.V., distributed by Elsevier (Amsterdam): 130 pp.
- Ziegler, P.A.**, (1990). *Geological Atlas of Western and Central Europe* (2nd edition). Shell Internationale Petroleum Maatschappij B.V; Geological Society Publishing House (Bath): 239 pp.
- Zijlstra, J.J.P.**, (1989). Reply on van der Weijden et al. *Geologie en Mijnbouw*, 68, p. 263-270
- Zijlstra, J.J.P.**, (1995). *The Sedimentology of Chalk*. Lecture Notes in Earth Sciences 54. ISBN 3-540- 58948-1.

Appendix A: Master log legend

	Skeletal fragments		Red Algae
	Belemnites		Bryozoans
	Foraminifera		Echinoderms
	Sponge spicules		Breccia
	Bioturbation		Flint concretions
	Unconformity		Mudclast
	Karst		Small fault
	Fossil layer		Shell bed
	Cross bedding		Lamination